

# Density Model for False Killer Whale (*Pseudorca crassidens*) for the U.S. East Coast: Supplementary Report

Model Version 2.1

Duke University Marine Geospatial Ecology Laboratory\*

2023-05-27


## Citation

When citing our methodology or results generally, please cite Roberts et al. (2016, 2023). The complete references appear at the end of this document. We are preparing a new article for a peer-reviewed journal that will eventually replace those. Until that is published, those are the best general citations.

When citing this model specifically, please use this reference:

Roberts JJ, Yack TM, Cañadas A, Fujioka E, Halpin PN, Barco SG, Boisseau O, Chavez-Rosales S, Cole TVN, Cotter MP, Cummings EW, Davis GE, DiGiovanni Jr. RA, Garrison LP, Gowan TA, Jackson KA, Kenney RD, Khan CB, Lockhart GG, Lomac-MacNair KS, McAlarney RJ, McLellan WA, Mullin KD, Nowacek DP, O'Brien O, Pabst DA, Palka DL, Quintana-Rizzo E, Redfern JV, Rickard ME, White M, Whitt AD, Zoidis AM (2022) Density Model for False Killer Whale (*Pseudorca crassidens*) for the U.S. East Coast, Version 2.1, 2023-05-27, and Supplementary Report. Marine Geospatial Ecology Laboratory, Duke University, Durham, North Carolina.

## Copyright and License

 This document and the accompanying results are © 2023 by the Duke University Marine Geospatial Ecology Laboratory and are licensed under a [Creative Commons Attribution 4.0 International License](https://creativecommons.org/licenses/by/4.0/).

## Model Version History

---

Version	Date	Description
1	2015-01-31	Initial version.
1.1	2015-05-14	Updated calculation of CVs. Switched density rasters to logarithmic breaks. No changes to the model.
1.2	2015-09-26	Updated the documentation. No changes to the model. Model files released as supplementary information to Roberts et al. (2016).

---

\*For questions or to offer feedback please contact Jason Roberts ([jason.roberts@duke.edu](mailto:jason.roberts@duke.edu)) and Tina Yack ([tina.yack@duke.edu](mailto:tina.yack@duke.edu))

*(continued)*

---

Version	Date	Description
2	2022-06-20	This model is a major update over the prior version, with substantial additional data, improved statistical methods, and an increased spatial resolution. It was released as part of the final delivery of the U.S. Navy Marine Species Density Database (NMSDD) for the Atlantic Fleet Testing and Training (AFTT) Phase IV Environmental Impact Statement. Several new collaborators joined and contributed survey data: New York State Department of Environmental Conservation, TetraTech, HDR, and Marine Conservation Research. We incorporated additional surveys from all continuing and new collaborators through the end of 2020. (Because some environmental covariates were only available through 2019, certain models only extend through 2019.) We increased the spatial resolution to 5 km and, at NOAA's request, we extended the model further inshore from New York through Maine. We reformulated and refitted all detection functions and spatial models. We updated all environmental covariates to newer products, when available, and added several covariates to the set of candidates. For models that incorporated dynamic covariates, we estimated model uncertainty using a new method that accounts for both model parameter error and temporal variability.
2.1	2023-05-27	Completed the supplementary report documenting the details of this model. Corrected the 5 and 95 percent rasters so that they contain the value 0 where the taxon was assumed absent, rather than NoData. Nothing else was changed.

---

# 1 Survey Data

We built this model from data collected between 1995-2020 (Table 1, Figure 1). We excluded surveys that did not target small cetaceans or were otherwise problematic for modeling them. We restricted the model to aerial survey transects with sea states of Beaufort 4 or less (for a few surveys we used Beaufort 3 or less) and shipboard transects with Beaufort 5 or less (for a few we used Beaufort 4 or less). We also excluded transects with poor weather or visibility for surveys that reported those conditions.

Table 1: Survey effort and observations considered for this model. Effort is tallied as the cumulative length of on-effort transects. Observations are the number of groups and individuals encountered while on effort. Off effort observations and those lacking an estimate of group size or distance to the group were excluded.

Institution	Program	Period	Effort	Observations		
			1000s km	Groups	Individuals	Mean Group Size
<b>Aerial Surveys</b>						
HDR	Navy Norfolk Canyon	2018-2019	11	0	0	
NEAq	CNM	2017-2020	2	0	0	
NEAq	MMS-WEA	2017-2020	37	0	0	
NEAq	NLPSC	2011-2015	43	0	0	
NEFSC	AMAPPS	2010-2019	83	0	0	
NEFSC	NARWSS	2003-2016	380	0	0	
NEFSC	Pre-AMAPPS	1999-2008	45	0	0	
NJDEP	NJEBS	2008-2009	9	0	0	
SEFSC	AMAPPS	2010-2020	112	0	0	
SEFSC	MATS	1995-2005	34	0	0	
SEFSC	SECAS	1995-1995	4	0	0	
UNCW	Navy Cape Hatteras	2011-2017	34	0	0	
UNCW	Navy Jacksonville	2009-2017	92	0	0	
UNCW	Navy Norfolk Canyon	2015-2017	14	0	0	
UNCW	Navy Onslow Bay	2007-2011	49	0	0	
VAMSC	MD DNR WEA	2013-2015	15	0	0	
VAMSC	Navy VACAPES	2016-2017	19	0	0	
VAMSC	VA CZM WEA	2012-2015	21	0	0	
		<b>Total</b>	<b>1,005</b>	<b>0</b>	<b>0</b>	
<b>Shipboard Surveys</b>						
MCR	SOTW Visual	2012-2019	8	1	1	1.0
NEFSC	AMAPPS	2011-2016	15	3	43	14.3
NEFSC	Pre-AMAPPS	1995-2007	16	1	23	23.0
SEFSC	AMAPPS	2011-2016	16	0	0	
SEFSC	Pre-AMAPPS	1998-2006	30	1	3	3.0
		<b>Total</b>	<b>85</b>	<b>6</b>	<b>70</b>	<b>11.7</b>
<b>Grand Total</b>			<b>1,091</b>	<b>6</b>	<b>70</b>	<b>11.7</b>

Table 2: Institutions that contributed surveys used in this model.

Institution	Full Name
HDR	HDR, Inc.
MCR	Marine Conservation Research
NEAq	New England Aquarium
NEFSC	NOAA Northeast Fisheries Science Center
NJDEP	New Jersey Department of Environmental Protection
SEFSC	NOAA Southeast Fisheries Science Center
UNCW	University of North Carolina Wilmington
VAMSC	Virginia Aquarium & Marine Science Center

Table 3: Descriptions and references for survey programs used in this model.

Program	Description	References
AMAPPS	Atlantic Marine Assessment Program for Protected Species	Palka et al. (2017), Palka et al. (2021)
CNM	Northeast Canyons Marine National Monument Aerial Surveys	Redfern et al. (2021)
MATS	Mid-Atlantic Tursiops Surveys	
MD DNR WEA	Aerial Surveys of the Maryland Wind Energy Area	Barco et al. (2015)
MMS-WEA	Marine Mammal Surveys of the MA and RI Wind Energy Areas	Quintana-Rizzo et al. (2021), O'Brien et al. (2022)
NARWSS	North Atlantic Right Whale Sighting Surveys	Cole et al. (2007)
Navy Cape Hatteras	Aerial Surveys of the Navy's Cape Hatteras Study Area	McLellan et al. (2018)
Navy Jacksonville	Aerial Surveys of the Navy's Jacksonville Study Area	Foley et al. (2019)
Navy Norfolk Canyon	Aerial Surveys of the Navy's Norfolk Canyon Study Area	Cotter (2019), McAlarney et al. (2018)
Navy Onslow Bay	Aerial Surveys of the Navy's Onslow Bay Study Area	Read et al. (2014)
Navy VACAPES	Aerial Survey Baseline Monitoring in the Continental Shelf Region of the VACAPES OPAREA	Mallette et al. (2017)
NJEBS	New Jersey Ecological Baseline Study	Geo-Marine, Inc. (2010), Whitt et al. (2015)
NLPSC	Northeast Large Pelagic Survey Collaborative Aerial Surveys	Leiter et al. (2017), Stone et al. (2017)
Pre-AMAPPS	Pre-AMAPPS Marine Mammal Abundance Surveys	Mullin and Fulling (2003), Garrison et al. (2010), Palka (2006)
SECAS	Southeast Cetacean Aerial Surveys	Blaylock and Hoggard (1994)
SOTW Visual	R/V Song of the Whale Visual Surveys	Ryan et al. (2013)
VA CZM WEA	Virginia CZM Wind Energy Area Surveys	Mallette et al. (2014), Mallette et al. (2015)



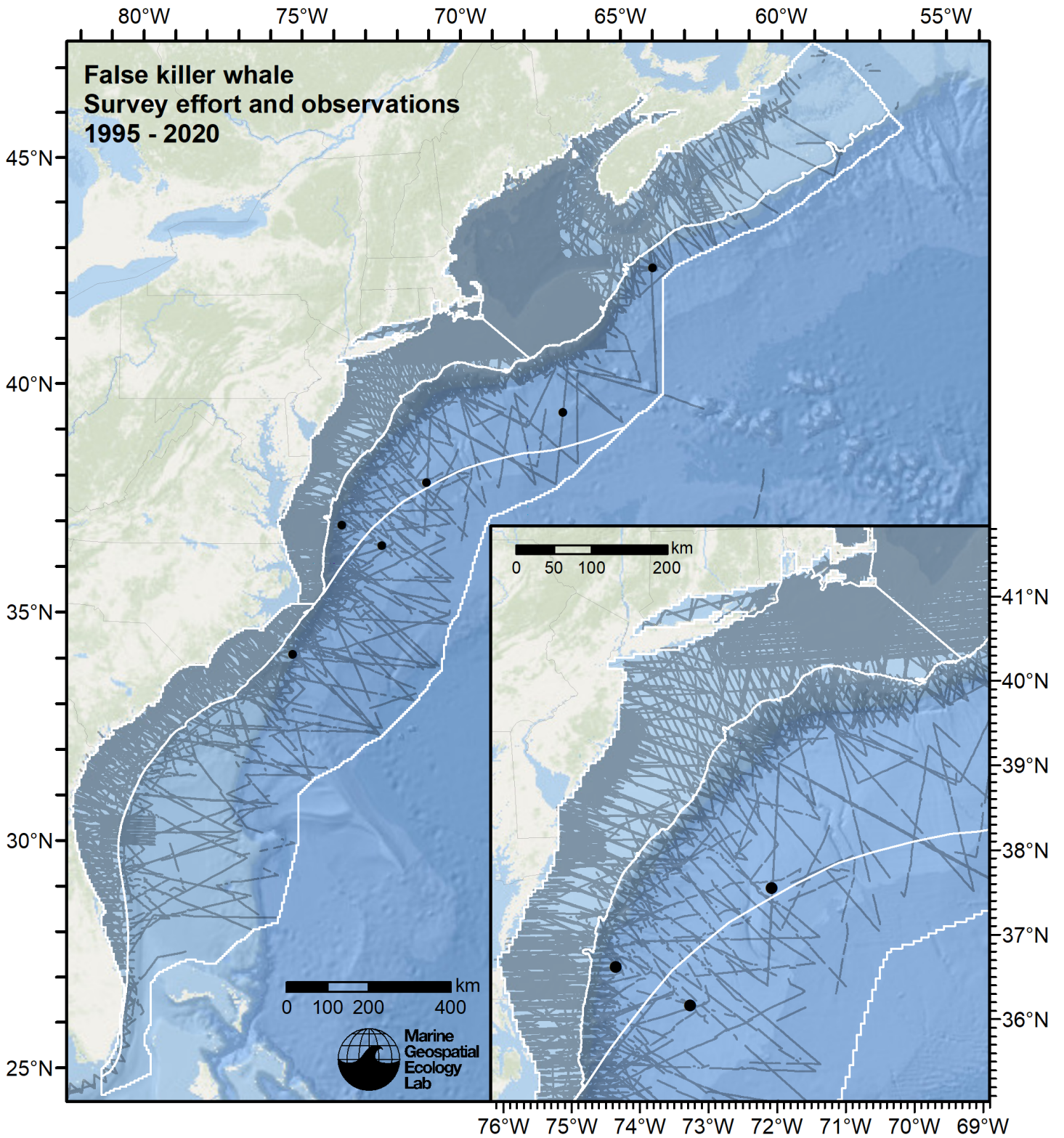


Figure 1: Survey effort and false killer whale observations available for density modeling, after detection functions were applied, and excluded segments and truncated observations were removed. White outlines show the strata for which density estimates were derived.

## 2 Detection Functions

### 2.1 Without a Taxonomic Covariate

We fitted the detection functions in this section to pools of species with similar detectability characteristics but could not use a taxonomic identification as a covariate to account for differences between them. We usually took this approach after trying the taxonomic covariate and finding it had insufficient statistical power to be retained. We also resorted to it when the focal taxon being modeled had too few observations to be allocated its own taxonomic covariate level and was too poorly known for us to confidently determine which other taxa we could group it with.



### 2.1.1.1 NEFSC Pre-AMAPPS

After right-truncating observations greater than 1300 m, we fitted the detection function to the 289 observations that remained (Table 4). The selected detection function (Figure 3) used a hazard rate key function with no covariates.

Table 4: Observations used to fit the NEFSC Pre-AMAPPS detection function.

ScientificName	n
Globicephala	148
Grampus griseus	141
<b>Total</b>	<b>289</b>

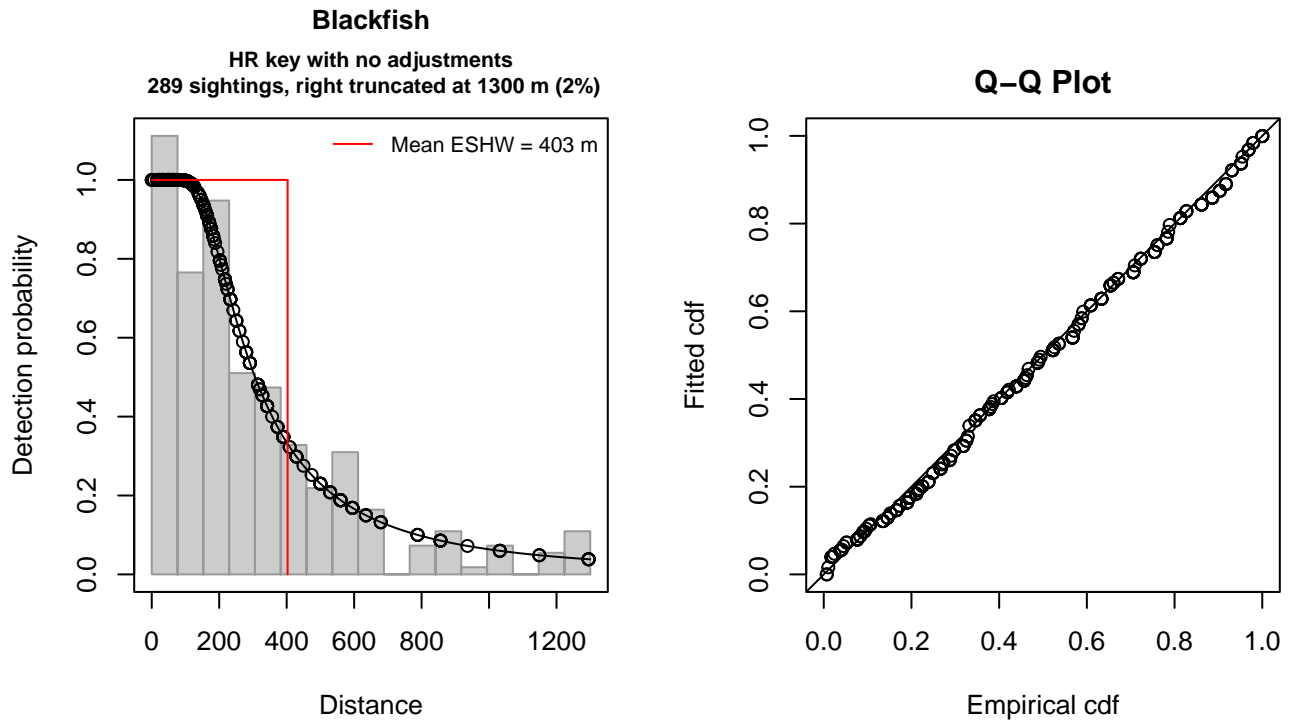


Figure 3: NEFSC Pre-AMAPPS detection function and Q-Q plot showing its goodness of fit.

Statistical output for this detection function:

```
Summary for ds object
Number of observations : 289
Distance range       : 0 - 1300
AIC                  : 3863.885
```

```
Detection function:
Hazard-rate key function
```

```
Detection function parameters
Scale coefficient(s):
      estimate      se
(Intercept) 5.540493 0.1221542
```

```
Shape coefficient(s):
      estimate      se
(Intercept) 0.6890237 0.1060228
```

	Estimate	SE	CV
Average p	0.3098149	0.02386401	0.07702667
N in covered region	932.8151840	85.09243937	0.09122111

Distance sampling Cramer-von Mises test (unweighted)  
 Test statistic = 0.049395 p = 0.879943

### 2.1.1.2 NEFSC AMAPPS Protocol

After right-truncating observations greater than 400 m, we fitted the detection function to the 164 observations that remained (Table 5). The selected detection function (Figure 4) used a hazard rate key function with Beaufort (Figure 5) as a covariate.

Table 5: Observations used to fit the NEFSC AMAPPS Protocol detection function.

ScientificName	n
Globicephala	76
Grampus griseus	87
Orcinus orca	1
<b>Total</b>	<b>164</b>

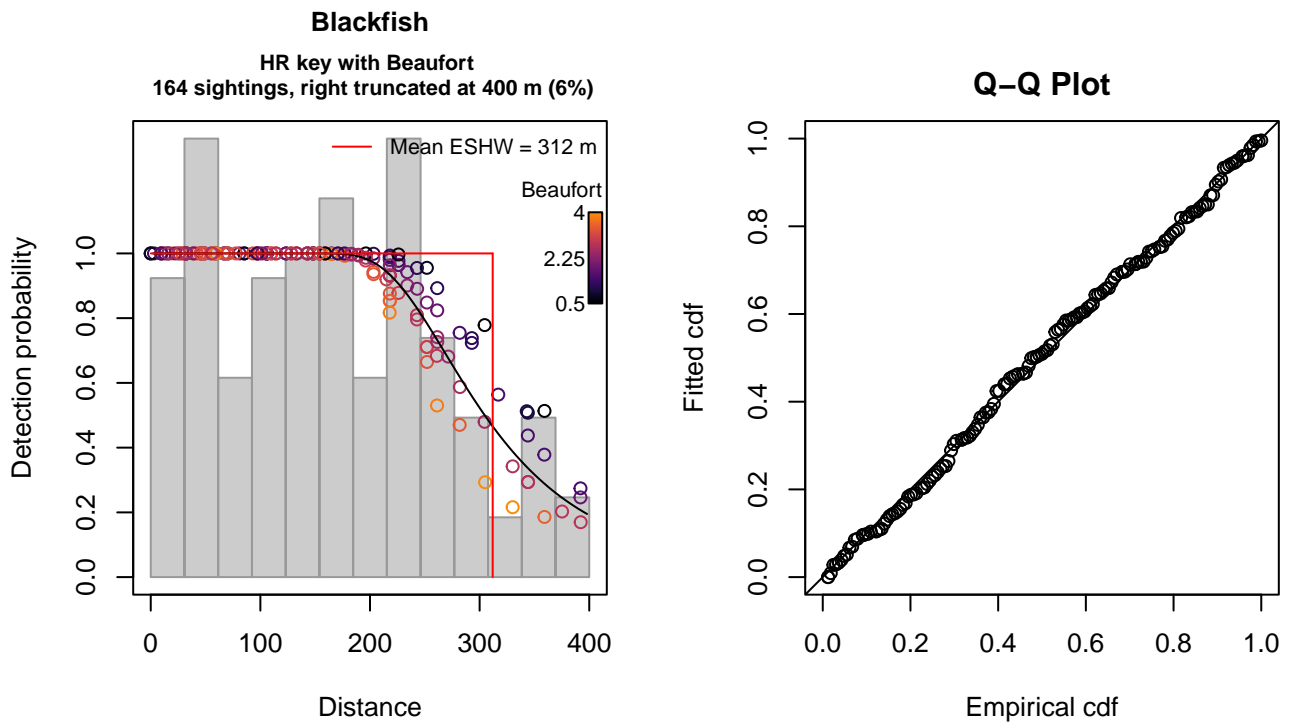


Figure 4: NEFSC AMAPPS Protocol detection function and Q-Q plot showing its goodness of fit.

Statistical output for this detection function:

```
Summary for ds object
Number of observations : 164
Distance range       : 0 - 400
AIC                  : 1943.903
```

```
Detection function:
Hazard-rate key function
```

```
Detection function parameters
```

Scale coefficient(s):  
                  estimate          se  
(Intercept) 5.85716562 0.18022637  
Beaufort -0.09331802 0.07079169

Shape coefficient(s):  
                  estimate          se  
(Intercept) 1.49927 0.3557806

	Estimate	SE	CV
Average p	0.7768428	0.04359073	0.05611268
N in covered region	211.1109209	14.20480094	0.06728596

Distance sampling Cramer-von Mises test (unweighted)  
Test statistic = 0.038316 p = 0.941631

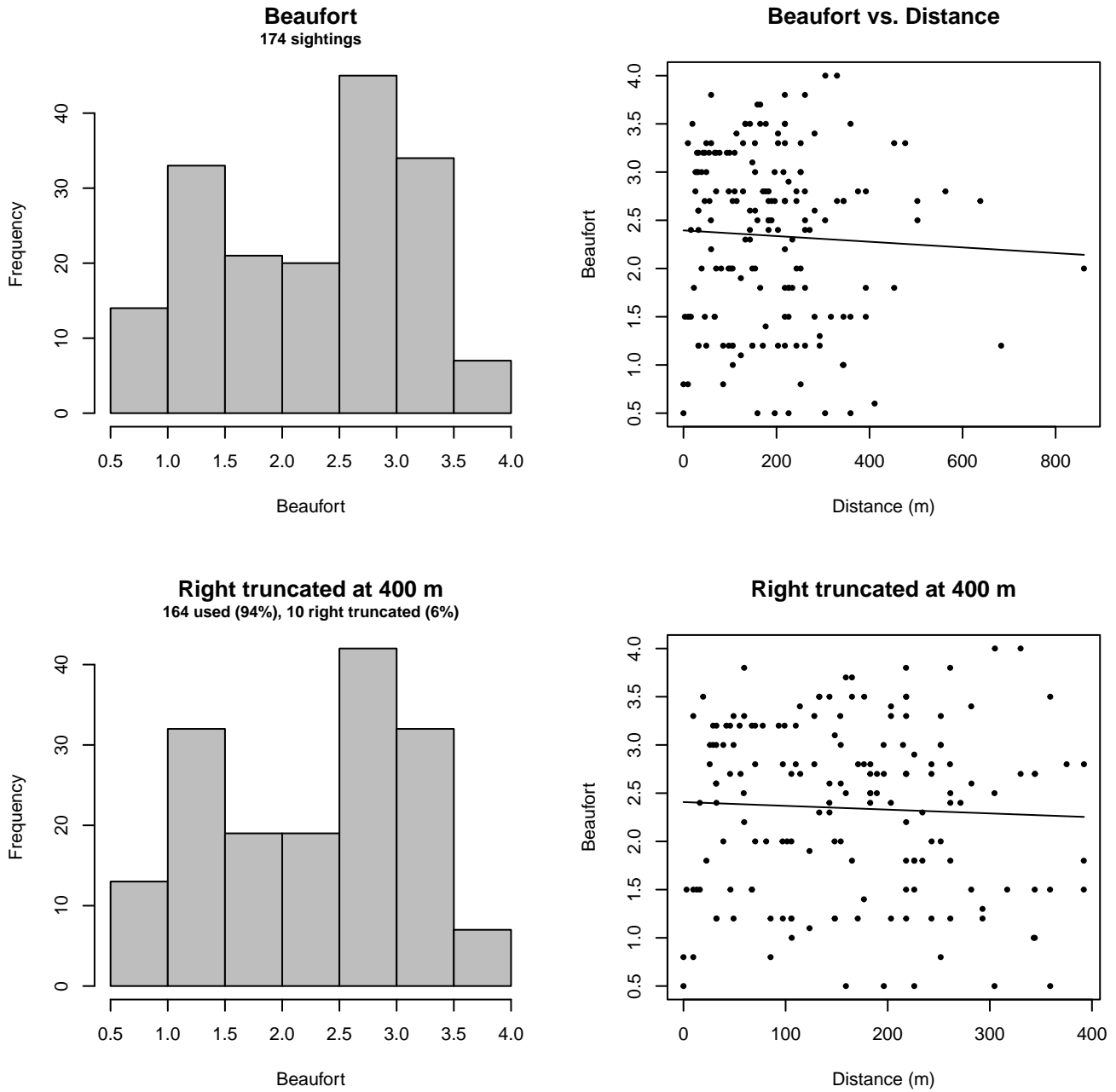


Figure 5: Distribution of the Beaufort covariate before (top row) and after (bottom row) observations were truncated to fit the NEFSC AMAPPS Protocol detection function.

### 2.1.1.3 SEFSC AMAPPS

After right-truncating observations greater than 400 m and left-truncating observations less than 50 m (Figure 7), we fitted the detection function to the 119 observations that remained (Table 6). The selected detection function (Figure 6) used a hazard rate key function with Beaufort (Figure 8) as a covariate.

Table 6: Observations used to fit the SEFSC AMAPPS detection function.

ScientificName	n
Globicephala	66
Grampus griseus	53
<b>Total</b>	<b>119</b>

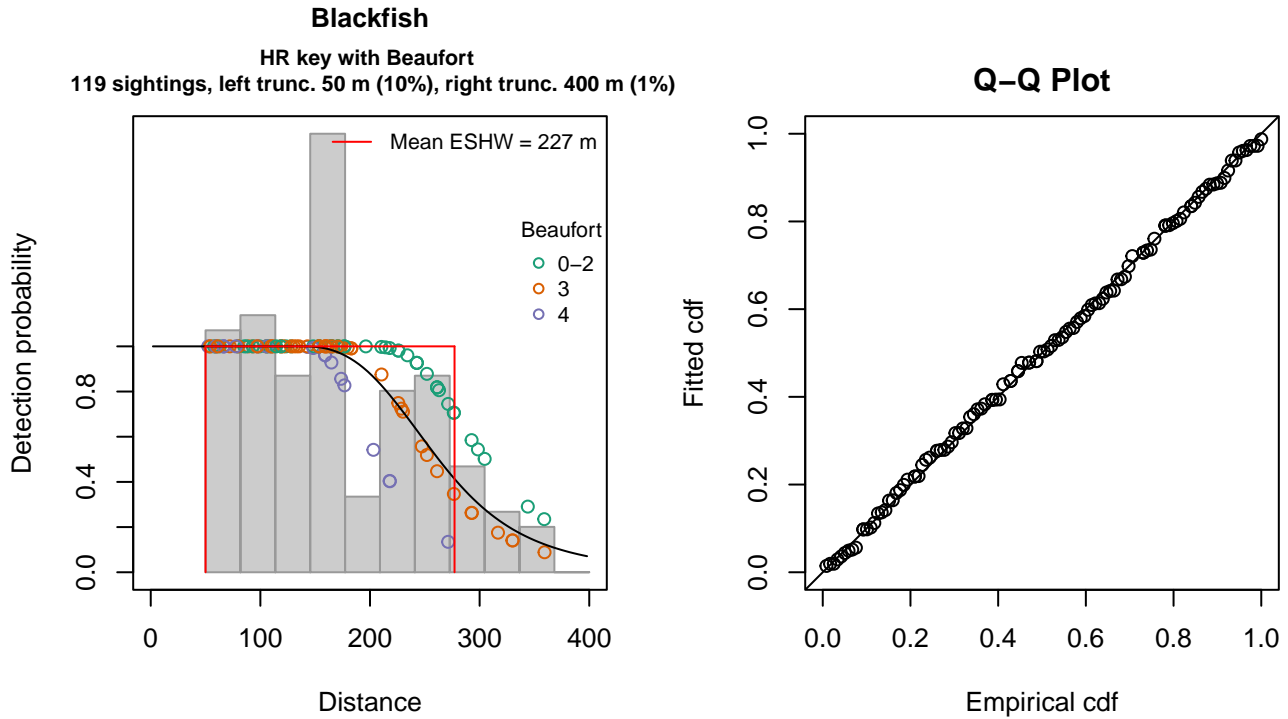


Figure 6: SEFSC AMAPPS detection function and Q-Q plot showing its goodness of fit.

Statistical output for this detection function:

Summary for ds object

Number of observations : 119  
 Distance range : 50 - 400  
 AIC : 1349.888

Detection function:

Hazard-rate key function

Detection function parameters

Scale coefficient(s):

	estimate	se
(Intercept)	5.6569520	0.1026861
Beaufort3	-0.1814855	0.1309136
Beaufort4	-0.3857171	0.1640754

Shape coefficient(s):

	estimate	se
(Intercept)	1.761805	0.3262538

	Estimate	SE	CV
Average p	0.6336189	0.04206604	0.06639012
N in covered region	187.8100597	16.38859266	0.08726153

Distance sampling Cramer-von Mises test (unweighted)

Test statistic = 0.019109 p = 0.997756



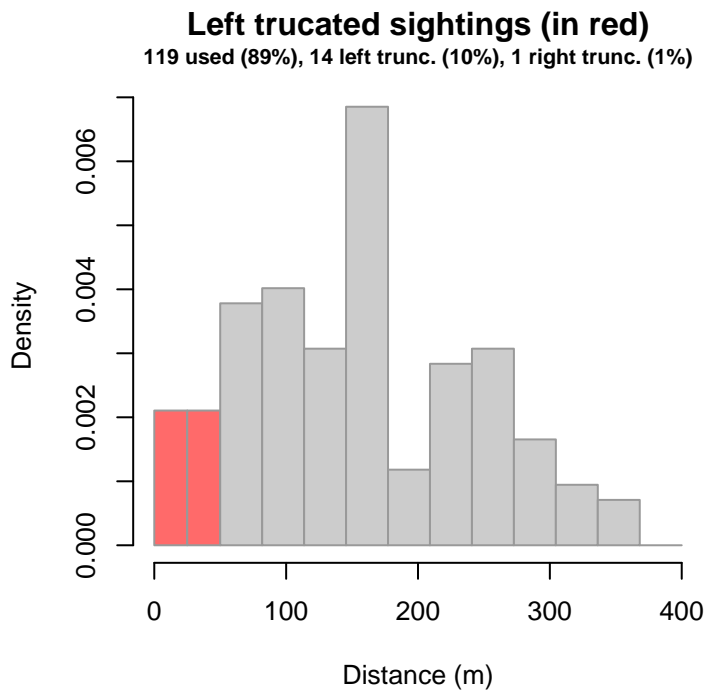


Figure 7: Density histogram of observations used to fit the SEFSC AMAPPS detection function, with the left-most bar showing observations at distances less than 50 m, which were left-truncated and excluded from the analysis [Buckland et al. (2001)]. (This bar may be very short if there were very few left-truncated sightings, or very narrow if the left truncation distance was very small; in either case it may not appear red.)

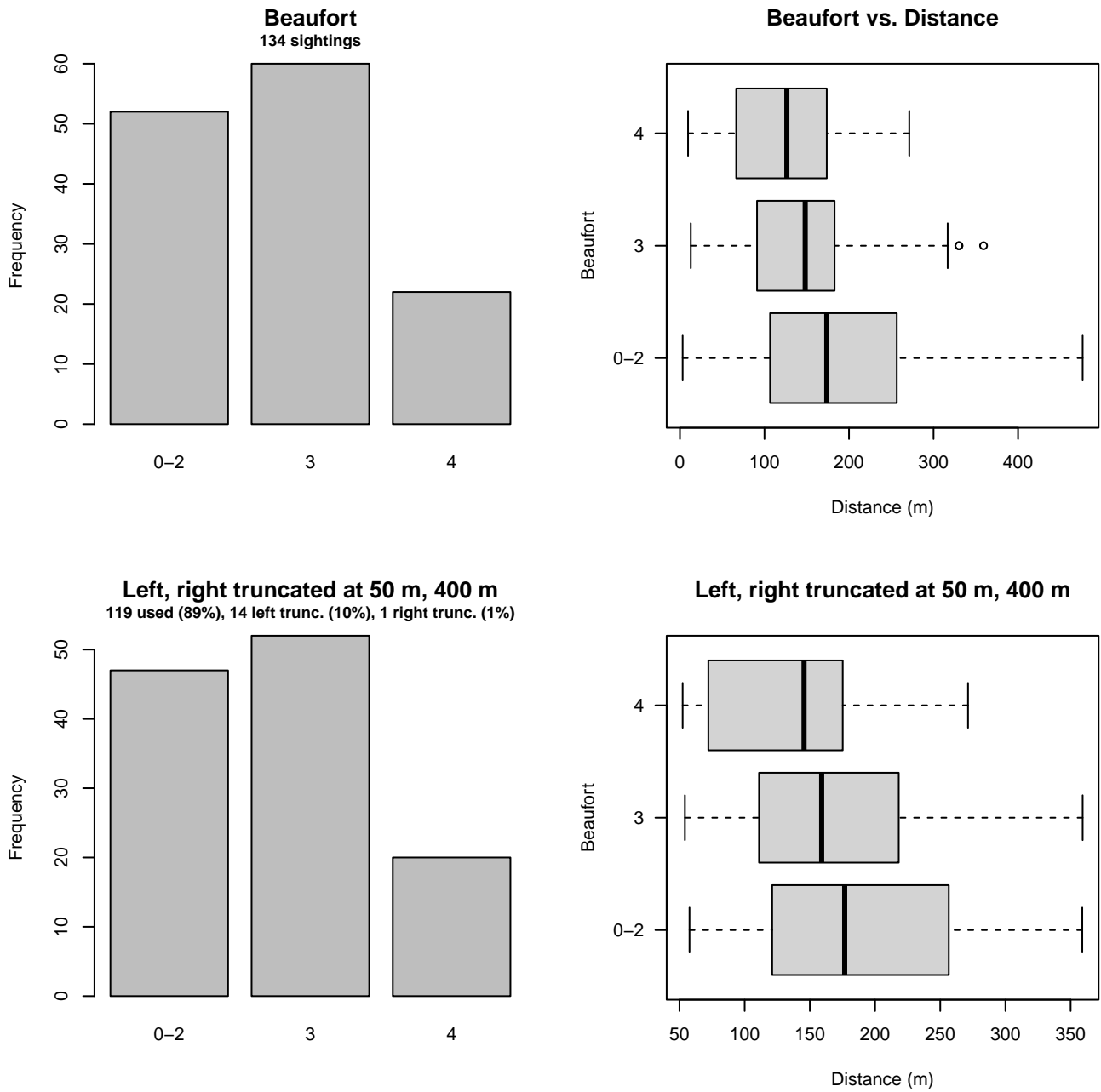


Figure 8: Distribution of the Beaufort covariate before (top row) and after (bottom row) observations were truncated to fit the SEFSC AMAPPS detection function.

#### 2.1.1.4 750 ft

After right-truncating observations greater than 629 m, we fitted the detection function to the 93 observations that remained (Table 7). The selected detection function (Figure 9) used a hazard rate key function with no covariates.

Table 7: Observations used to fit the 750 ft detection function.

ScientificName	n
Feresa attenuata	3
Feresa attenuata/Peponocephala electra	7
Globicephala	12
Grampus griseus	69
Pseudorca crassidens	2
<b>Total</b>	<b>93</b>

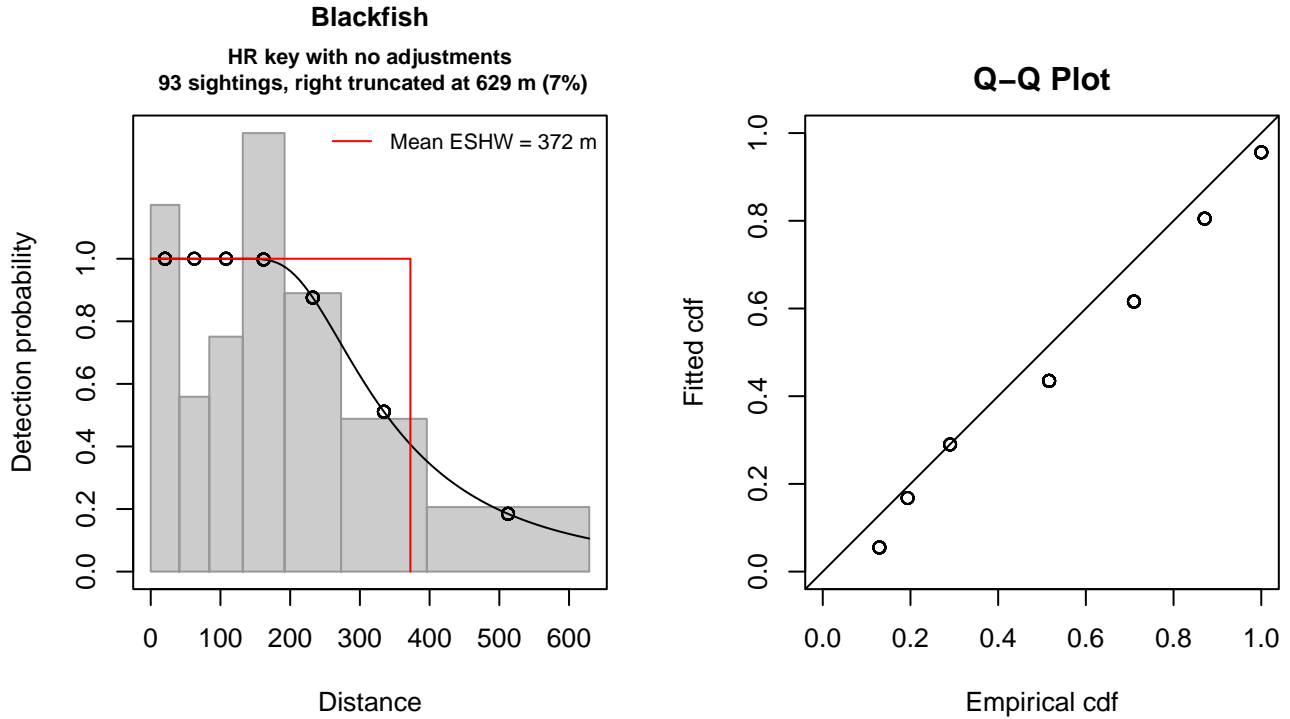


Figure 9: 750 ft detection function and Q-Q plot showing its goodness of fit.

Statistical output for this detection function:

Summary for ds object

Number of observations : 93  
 Distance range : 0 - 629  
 AIC : 359.4726

Detection function:

Hazard-rate key function

Detection function parameters

Scale coefficient(s):  
 estimate se  
 (Intercept) 5.698811 0.1702564

Shape coefficient(s):  
 estimate se  
 (Intercept) 1.07856 0.3654486

	Estimate	SE	CV
Average p	0.5920954	0.06138719	0.1036779

N in covered region 157.0692704 19.32345801 0.1230251

Distance sampling Cramer-von Mises test (unweighted)  
Test statistic = 0.271977 p = 0.162483

### 2.1.1.5 NARWSS 2003-2016

After right-truncating observations greater than 2905 m, we fitted the detection function to the 485 observations that remained (Table 8). The selected detection function (Figure 10) used a hazard rate key function with Beaufort (Figure 11) as a covariate.

Table 8: Observations used to fit the NARWSS 2003-2016 detection function.

ScientificName	n
Globicephala	376
Grampus griseus	106
Orcinus orca	3
<b>Total</b>	<b>485</b>

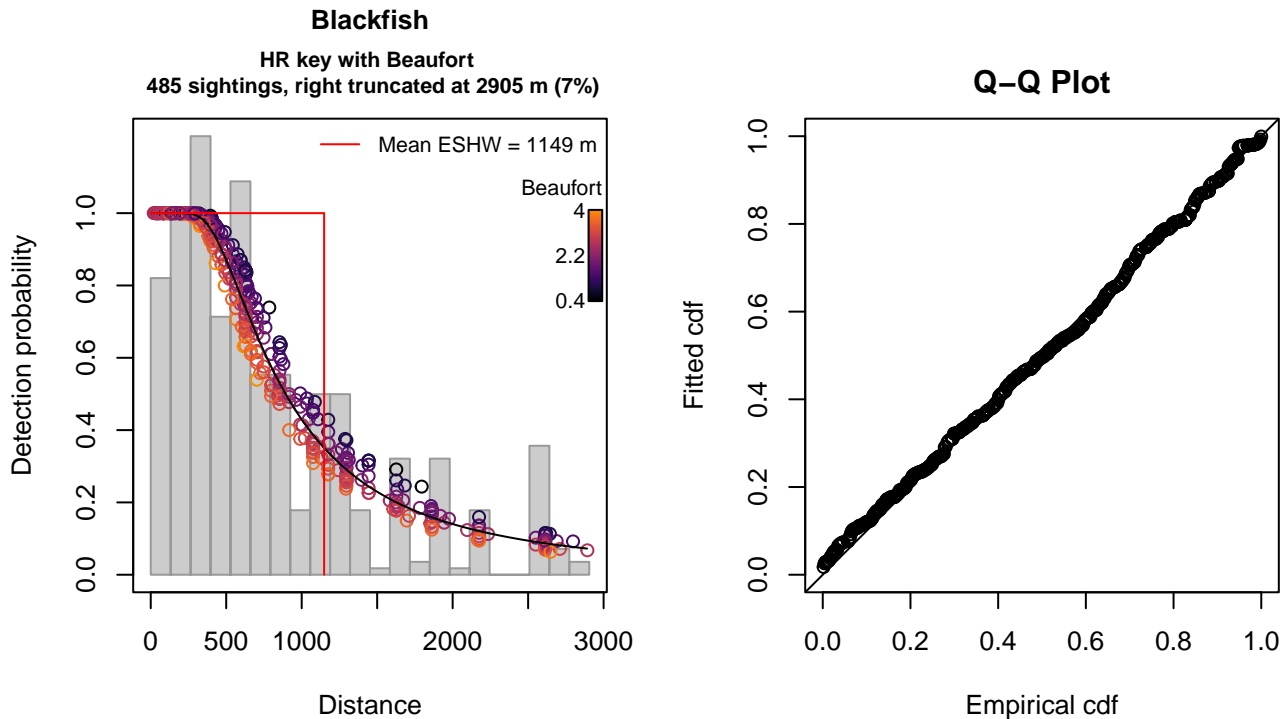


Figure 10: NARWSS 2003-2016 detection function and Q-Q plot showing its goodness of fit.

Statistical output for this detection function:

```
Summary for ds object
Number of observations : 485
Distance range       : 0 - 2905
AIC                  : 7420.46
```

```
Detection function:
Hazard-rate key function
```

```
Detection function parameters
Scale coefficient(s):
```

	estimate	se
(Intercept)	6.8787415	0.22789350
Beaufort	-0.1141738	0.08537414

Shape coefficient(s):

	estimate	se
(Intercept)	0.6421837	0.09908371

	Estimate	SE	CV
Average p	0.393189	0.02454407	0.06242307
N in covered region	1233.503530	88.54090900	0.07178002

Distance sampling Cramer-von Mises test (unweighted)

Test statistic = 0.097833 p = 0.595605

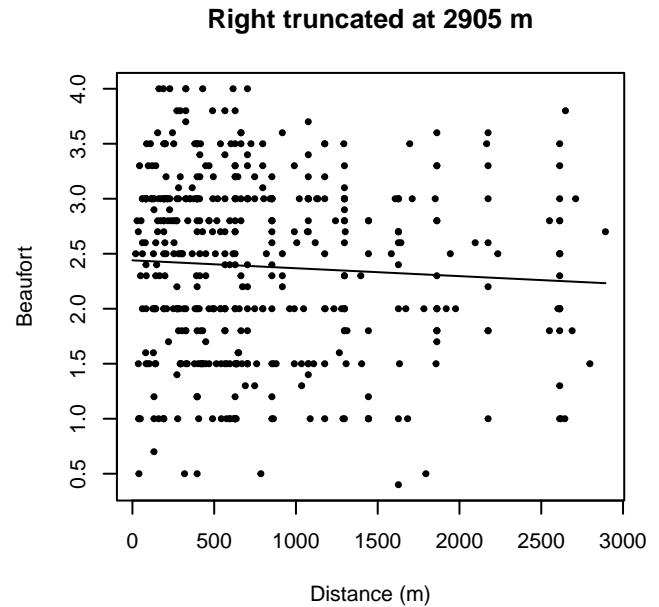
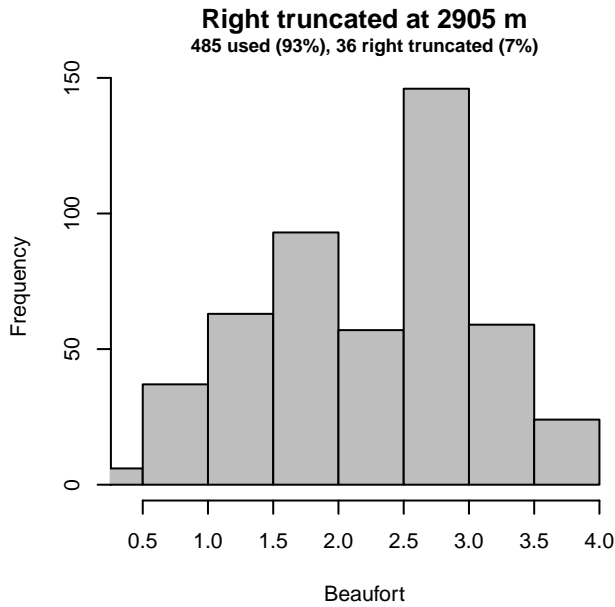
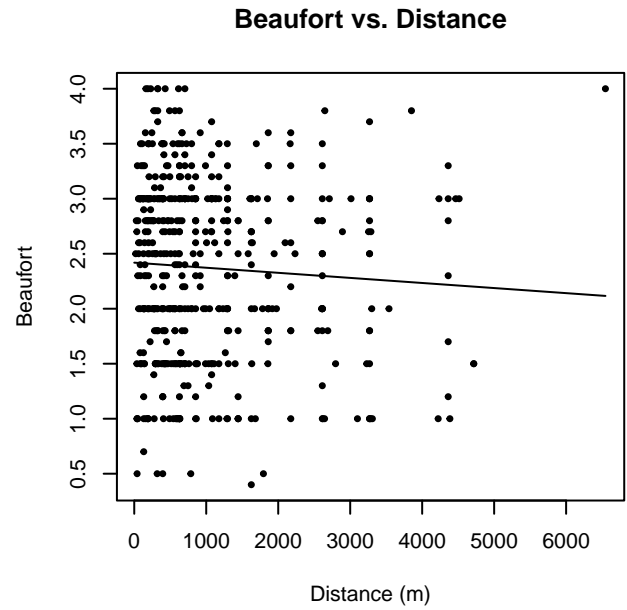
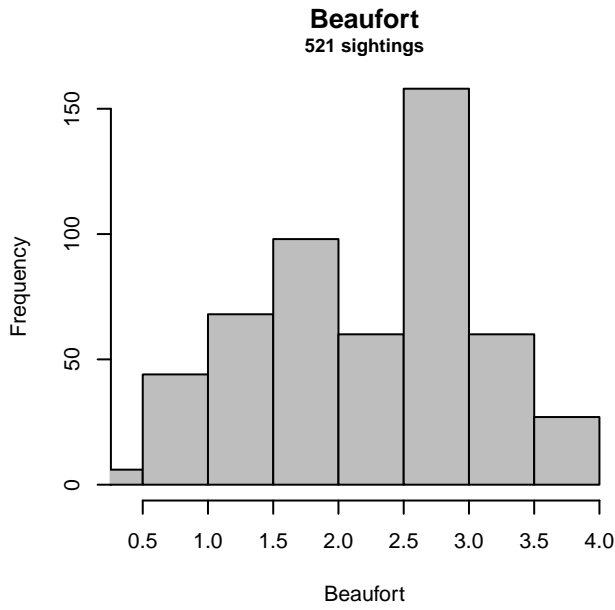


Figure 11: Distribution of the Beaufort covariate before (top row) and after (bottom row) observations were truncated to fit the NARWSS 2003-2016 detection function.

### 2.1.1.6 NEAq New England

After right-truncating observations greater than 1852 m and left-truncating observations less than 71 m (Figure 13), we fitted the detection function to the 58 observations that remained (Table 9). The selected detection function (Figure 12) used a half normal key function with no covariates.

Table 9: Observations used to fit the NEAq New England detection function.

ScientificName	n
Globicephala	16
Grampus griseus	42
<b>Total</b>	<b>58</b>

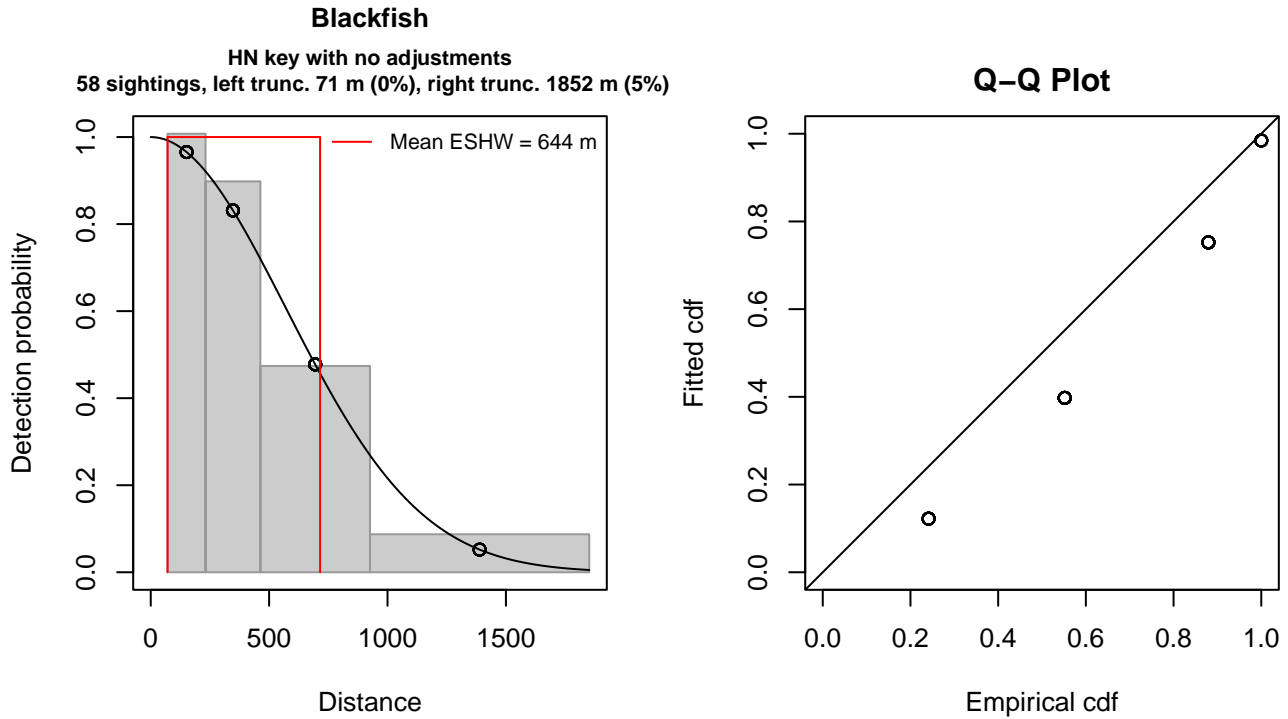


Figure 12: NEAq New England detection function and Q-Q plot showing its goodness of fit.

Statistical output for this detection function:

Summary for ds object

Number of observations : 58  
 Distance range : 71 - 1852  
 AIC : 156.0466

Detection function:

Half-normal key function

Detection function parameters

Scale coefficient(s):

	estimate	se
(Intercept)	6.347853	0.1032999

	Estimate	SE	CV
Average p	0.3617668	0.04089634	0.1130461
N in covered region	160.3242530	24.72501947	0.1542188

Distance sampling Cramer-von Mises test (unweighted)

Test statistic = 0.430759 p = 0.060002

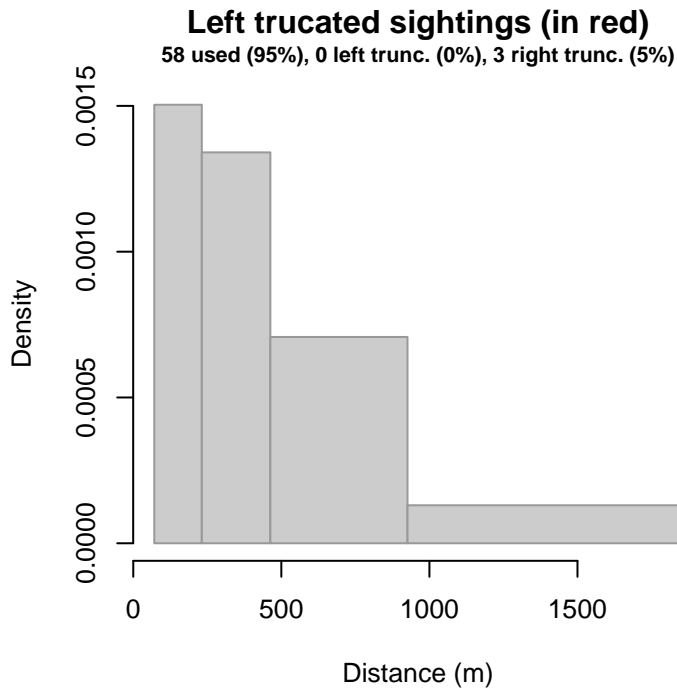


Figure 13: Density histogram of observations used to fit the NEAq New England detection function, with the left-most bar showing observations at distances less than 71 m, which were left-truncated and excluded from the analysis [Buckland et al. (2001)]. (This bar may be very short if there were very few left-truncated sightings, or very narrow if the left truncation distance was very small; in either case it may not appear red.)

### 2.1.1.7 UNCW Navy and VAMSC

After right-truncating observations greater than 1300 m, we fitted the detection function to the 312 observations that remained (Table 10). The selected detection function (Figure 14) used a hazard rate key function with Visibility (Figure 15) as a covariate.

Table 10: Observations used to fit the UNCW Navy and VAMSC detection function.

ScientificName	n
Globicephala macrorhynchus	223
Grampus griseus	88
Peponocephala electra	1
<b>Total</b>	<b>312</b>



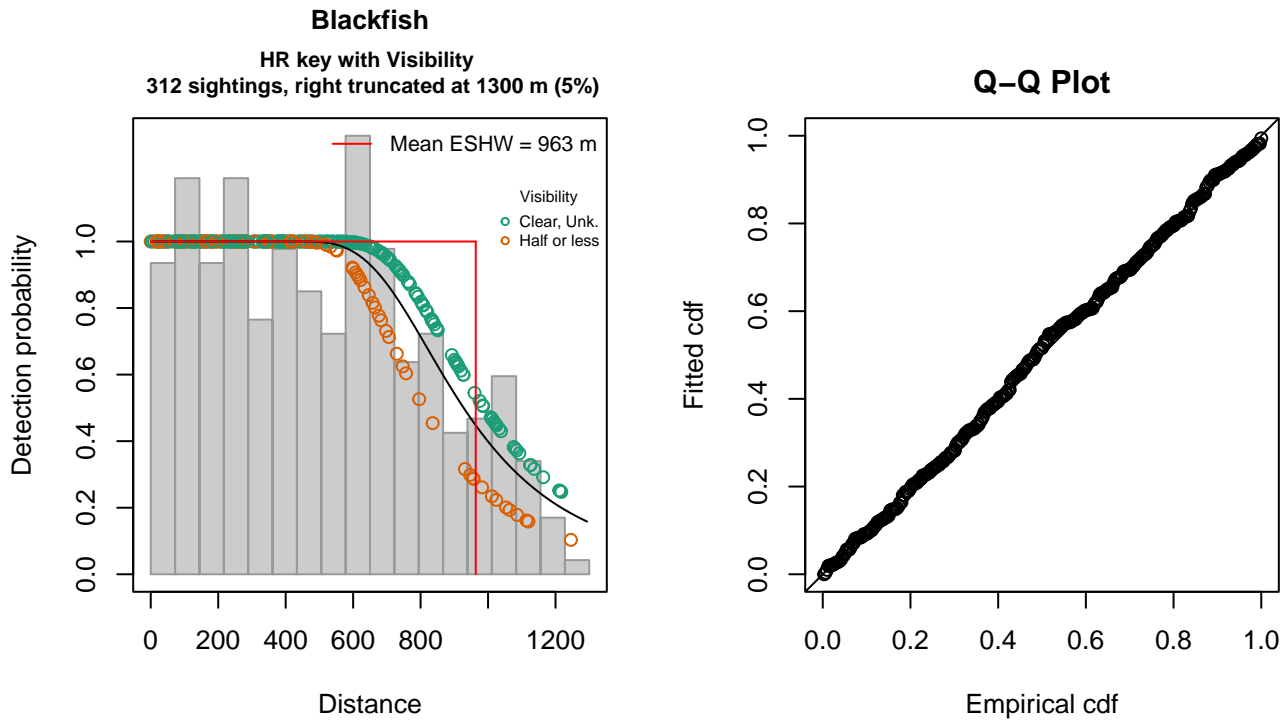


Figure 14: UNCW Navy and VAMSC detection function and Q-Q plot showing its goodness of fit.

Statistical output for this detection function:

Summary for ds object

Number of observations : 312  
 Distance range : 0 - 1300  
 AIC : 4410.896

Detection function:

Hazard-rate key function

Detection function parameters

Scale coefficient(s):

	estimate	se
(Intercept)	6.8110764	0.06588732
VisibilityHalf or less	-0.1997402	0.10267594

Shape coefficient(s):

	estimate	se
(Intercept)	1.45681	0.2585487

	Estimate	SE	CV
Average p	0.7368436	0.03057513	0.04149473
N in covered region	423.4277360	21.50283164	0.05078277

Distance sampling Cramer-von Mises test (unweighted)

Test statistic = 0.030099 p = 0.975843

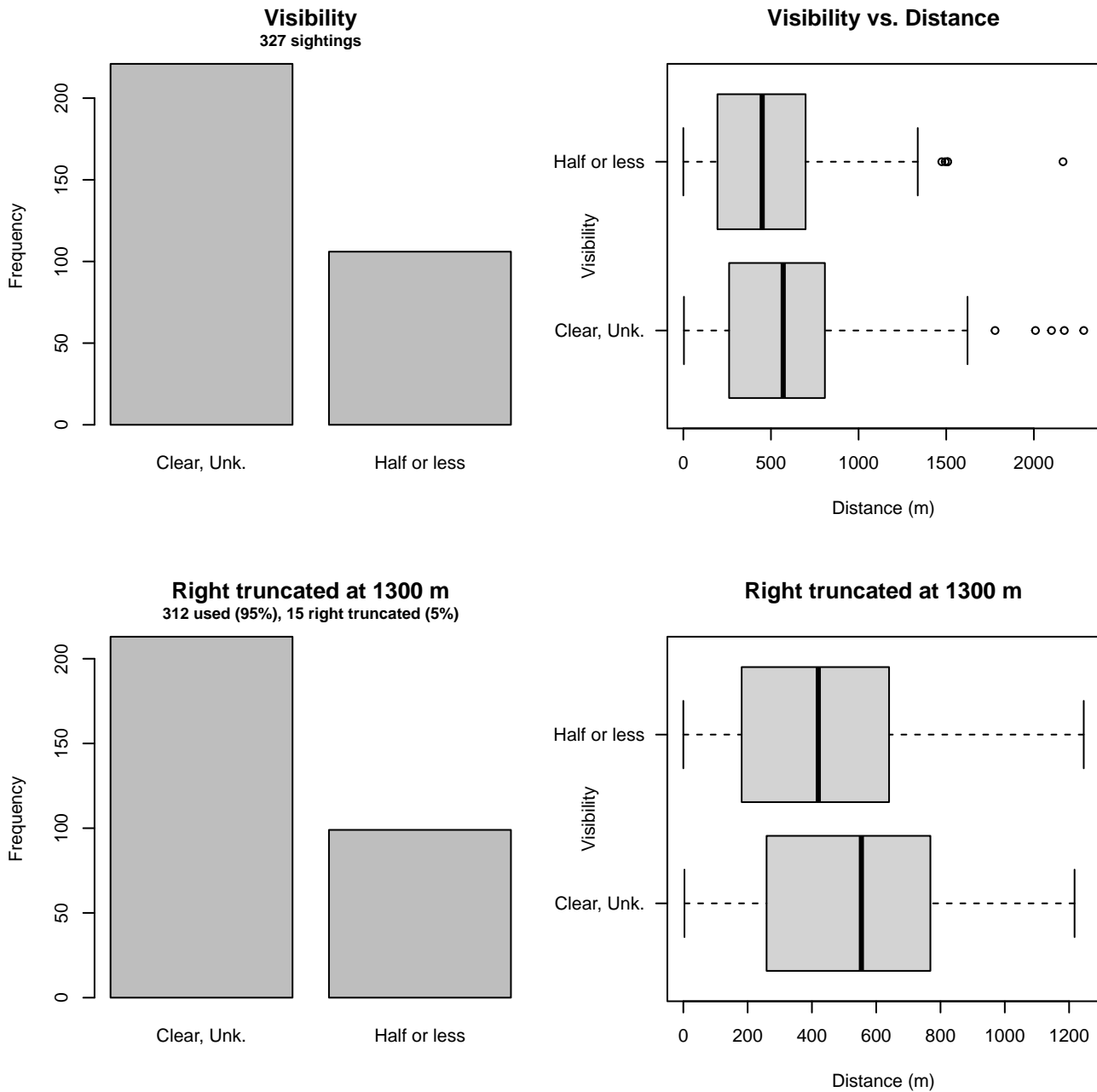


Figure 15: Distribution of the Visibility covariate before (top row) and after (bottom row) observations were truncated to fit the UNCW Navy and VAMSC detection function.

### 2.1.1.8 HDR

After right-truncating observations greater than 1500 m and left-truncating observations less than 111 m (Figure 17), we fitted the detection function to the 108 observations that remained (Table 11). The selected detection function (Figure 16) used a hazard rate key function with Swell (Figure 18) as a covariate.

Table 11: Observations used to fit the HDR detection function.

ScientificName	n
Globicephala	66
Grampus griseus	42
<b>Total</b>	<b>108</b>

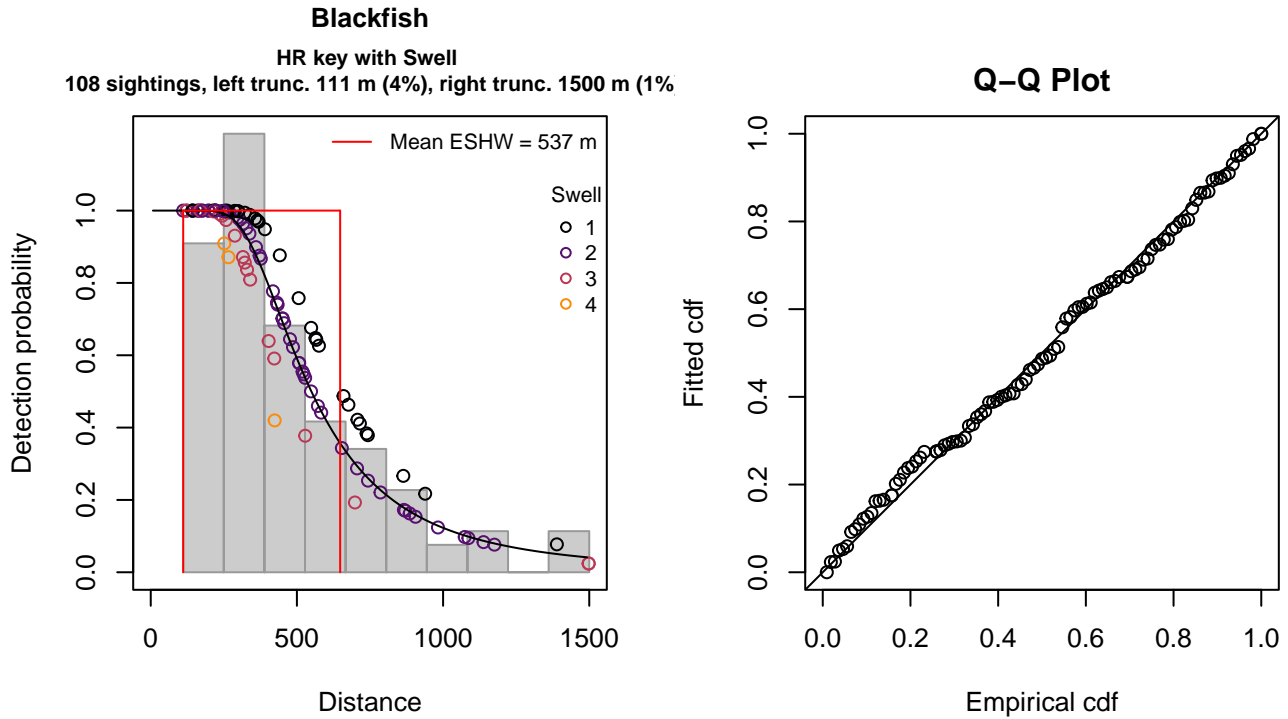


Figure 16: HDR detection function and Q-Q plot showing its goodness of fit.

Statistical output for this detection function:

Summary for ds object

Number of observations : 108  
 Distance range : 111 - 1500  
 AIC : 1479.102

Detection function:

Hazard-rate key function

Detection function parameters

Scale coefficient(s):

	estimate	se
(Intercept)	6.5207075	0.2852850
Swell	-0.1712662	0.1474231

Shape coefficient(s):

	estimate	se
(Intercept)	1.044626	0.1820091

	Estimate	SE	CV
Average p	0.3789427	0.04750114	0.1253518
N in covered region	285.0035382	41.82280744	0.1467449

Distance sampling Cramer-von Mises test (unweighted)

Test statistic = 0.045799 p = 0.901252

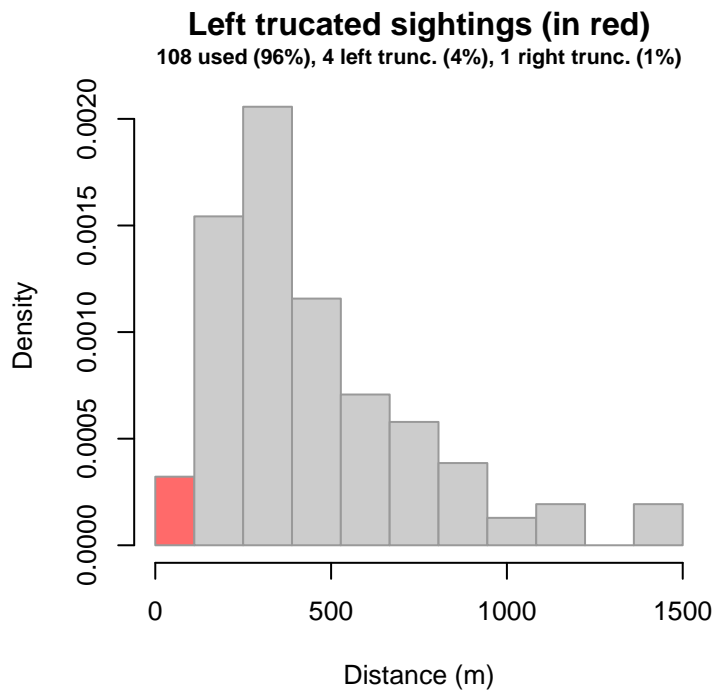


Figure 17: Density histogram of observations used to fit the HDR detection function, with the left-most bar showing observations at distances less than 111 m, which were left-truncated and excluded from the analysis [Buckland et al. (2001)]. (This bar may be very short if there were very few left-truncated sightings, or very narrow if the left truncation distance was very small; in either case it may not appear red.)

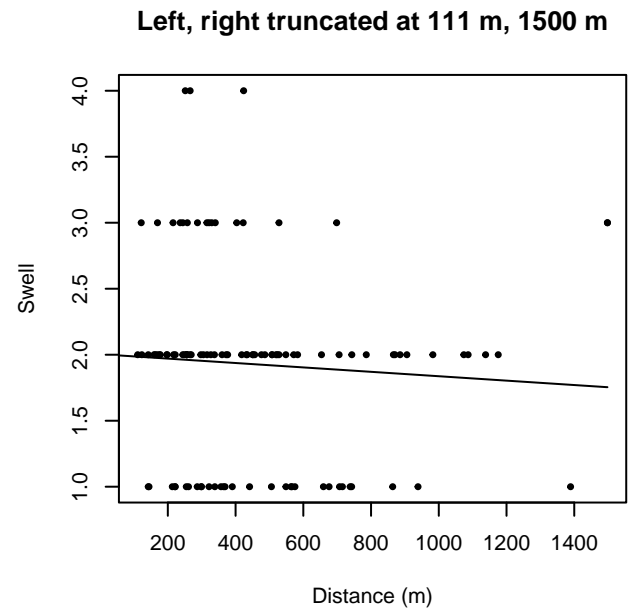
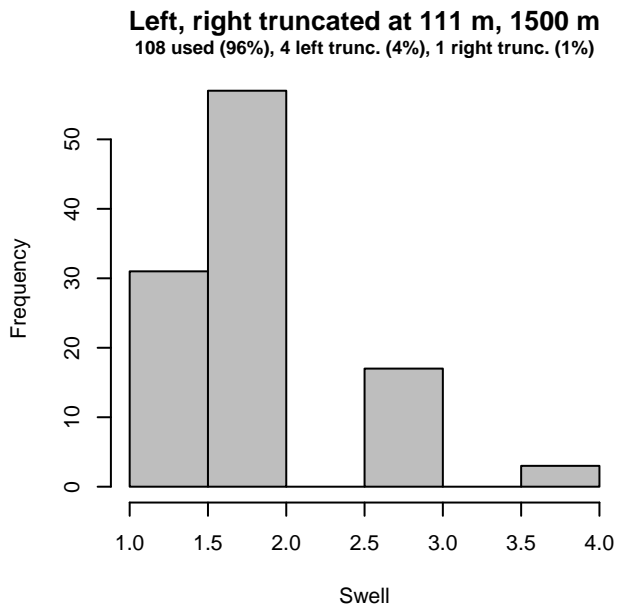
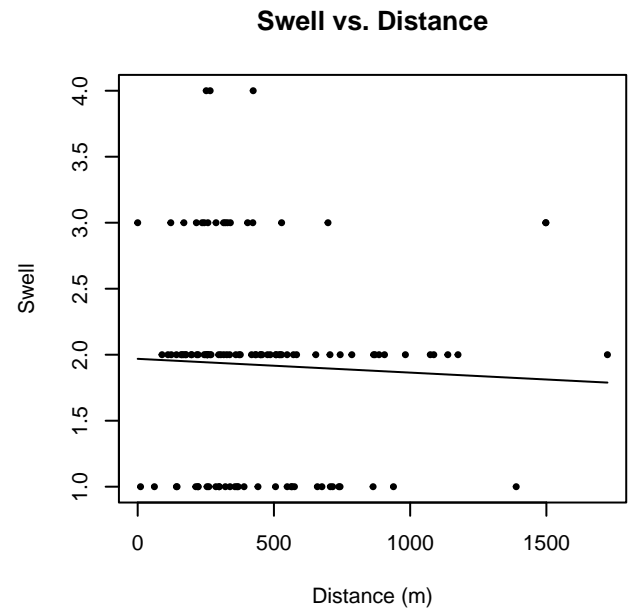
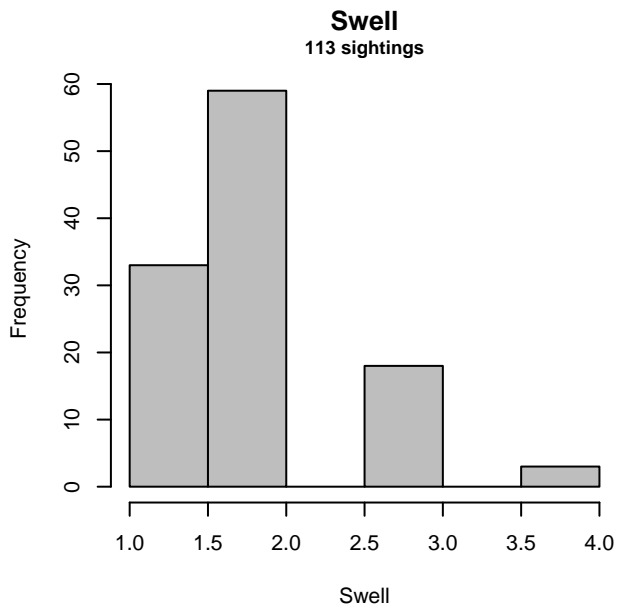


Figure 18: Distribution of the Swell covariate before (top row) and after (bottom row) observations were truncated to fit the HDR detection function.

## 2.1.2 Shipboard Surveys

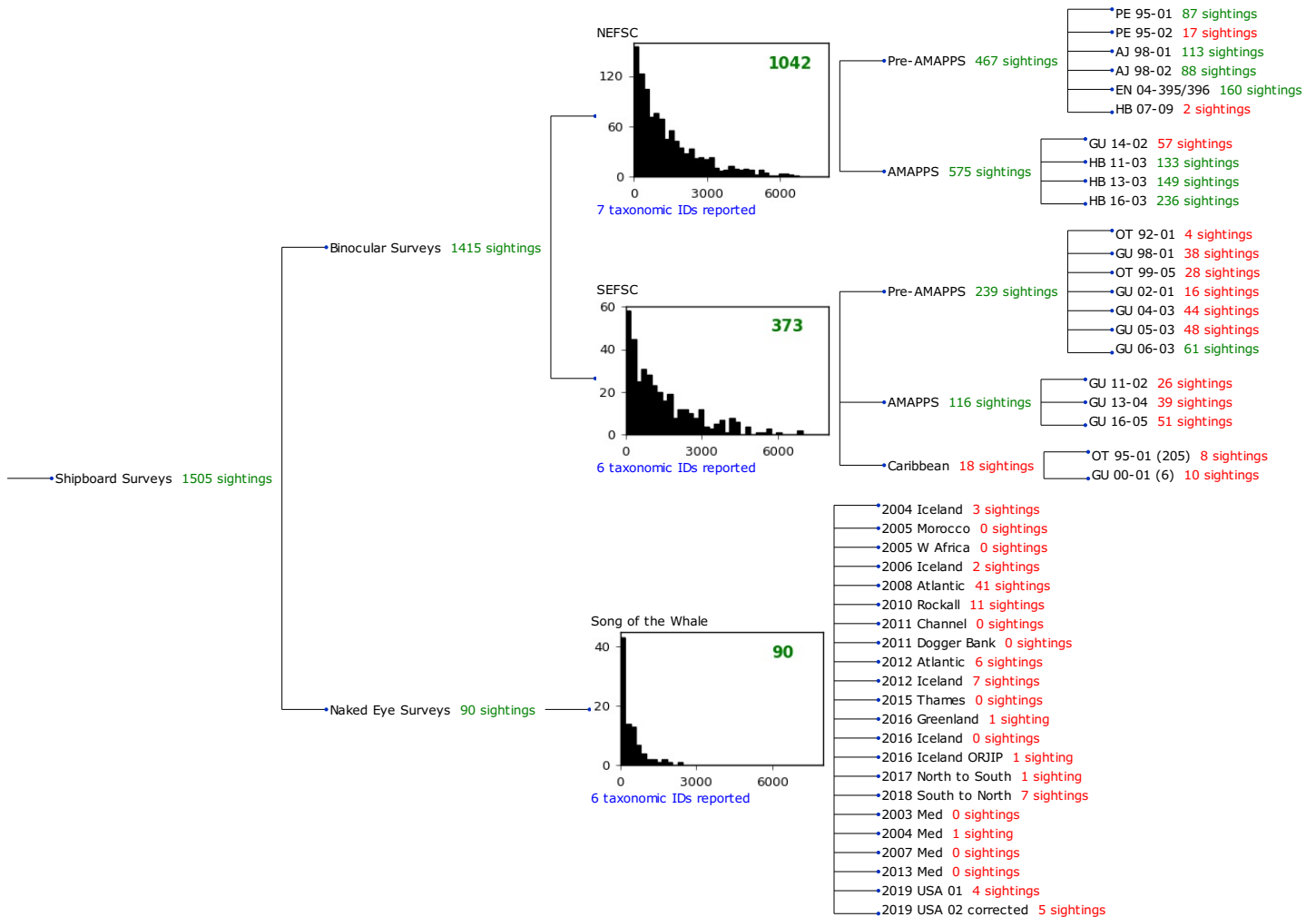


Figure 19: Detection hierarchy for shipboard surveys, showing how they were pooled during detectability modeling, for detection functions that pooled multiple taxa but could not use a taxonomic covariate to account for differences between them. Each histogram represents a detection function and summarizes the perpendicular distances of observations that were pooled to fit it, prior to truncation. Observation counts, also prior to truncation, are shown in green when they met the recommendation of Buckland et al. (2001) that detection functions utilize at least 60 sightings, and red otherwise. For rare taxa, it was not always possible to meet this recommendation, yielding higher statistical uncertainty. During the spatial modeling stage of the analysis, effective strip widths were computed for each survey using the closest detection function above it in the hierarchy (i.e. moving from right to left in the figure). Surveys that do not have a detection function above them in this figure were either addressed by a detection function presented in a different section of this report, or were omitted from the analysis.

### 2.1.2.1 NEFSC

After right-truncating observations greater than 6500 m, we fitted the detection function to the 1038 observations that remained (Table 12). The selected detection function (Figure 20) used a hazard rate key function with Beaufort (Figure 21), Program (Figure 22) and VesselName (Figure 23) as covariates.

Table 12: Observations used to fit the NEFSC detection function.

ScientificName	n
Feresa attenuata	1
Globicephala	339
Globicephala macrorhynchus	3
Globicephala melas	2
Grampus griseus	687
Orcinus orca	2
Pseudorca crassidens	4
<b>Total</b>	<b>1038</b>

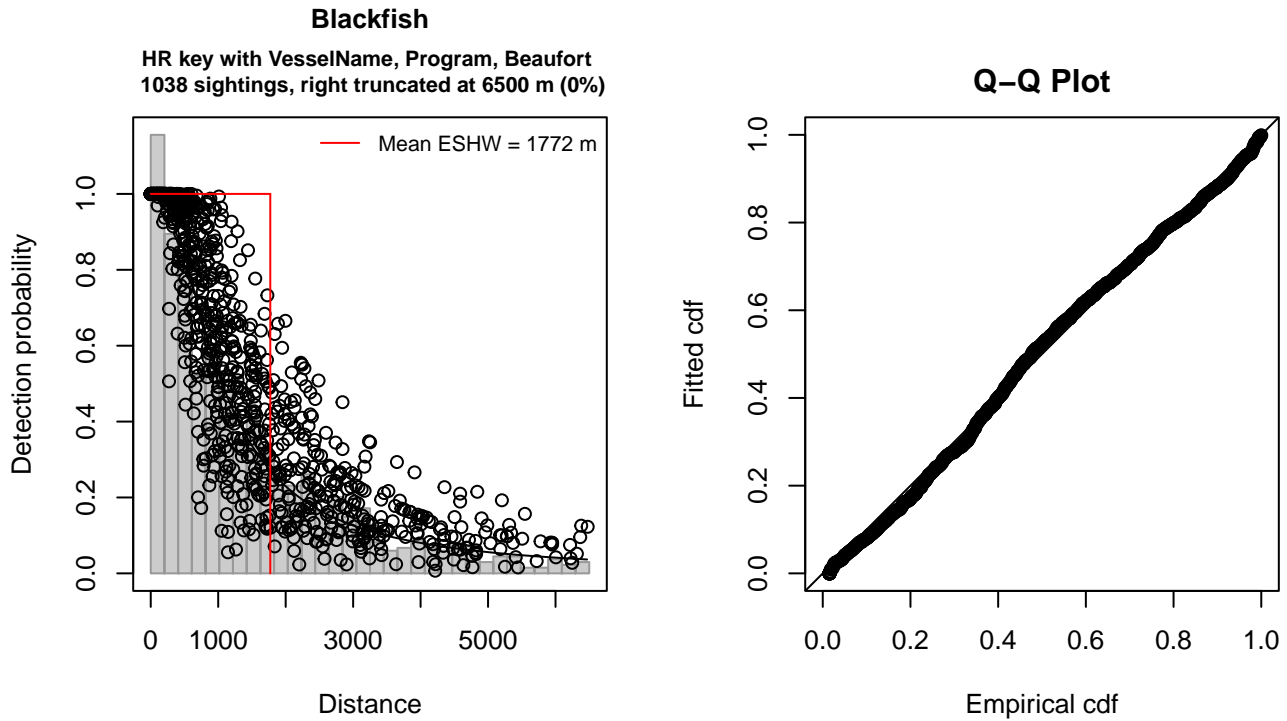


Figure 20: NEFSC detection function and Q-Q plot showing its goodness of fit.

Statistical output for this detection function:

Summary for ds object

Number of observations : 1038  
 Distance range : 0 - 6500  
 AIC : 17099.06

Detection function:

Hazard-rate key function

Detection function parameters

Scale coefficient(s):

	estimate	se
(Intercept)	7.9293942	0.15761667
VesselNameGunter	-0.8354128	0.20812306
VesselNamePelican	-0.3342984	0.17874334
ProgramMarine Mammal Abundance Surveys	-0.2436275	0.10871377
Beaufort	-0.3461133	0.05534466

Shape coefficient(s):

	estimate	se
(Intercept)	0.5332413	0.05606824

	Estimate	SE	CV
Average p	0.2418497	0.01240714	0.05130104
N in covered region	4291.9212516	249.96005128	0.05823966

Distance sampling Cramer-von Mises test (unweighted)

Test statistic = 0.293125 p = 0.141354

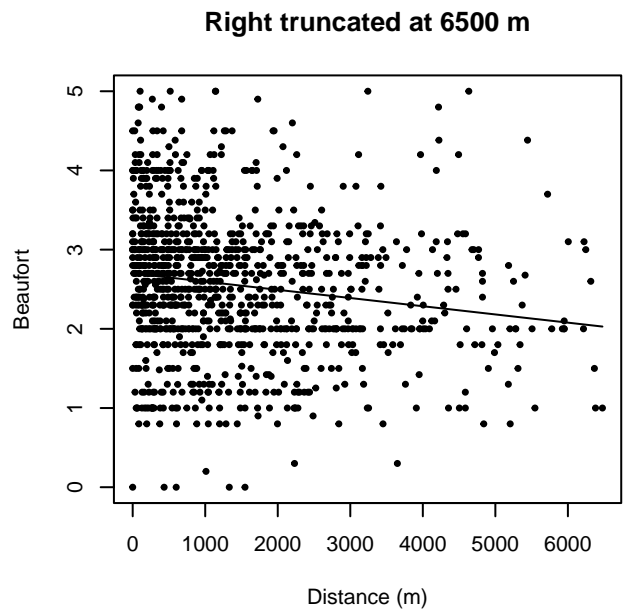
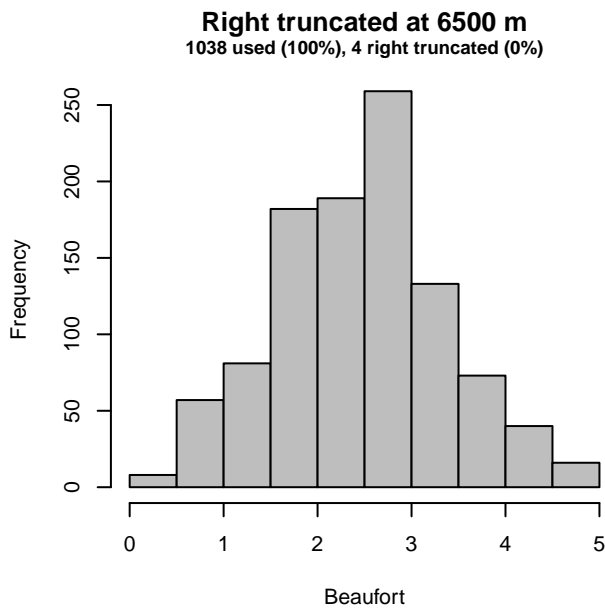
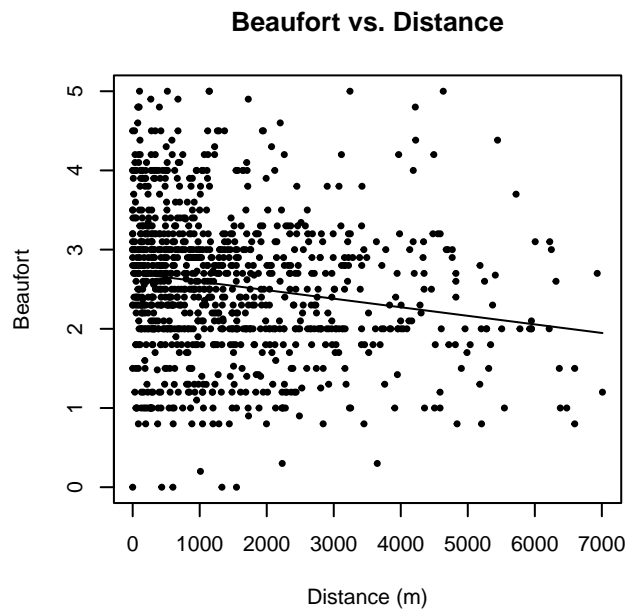
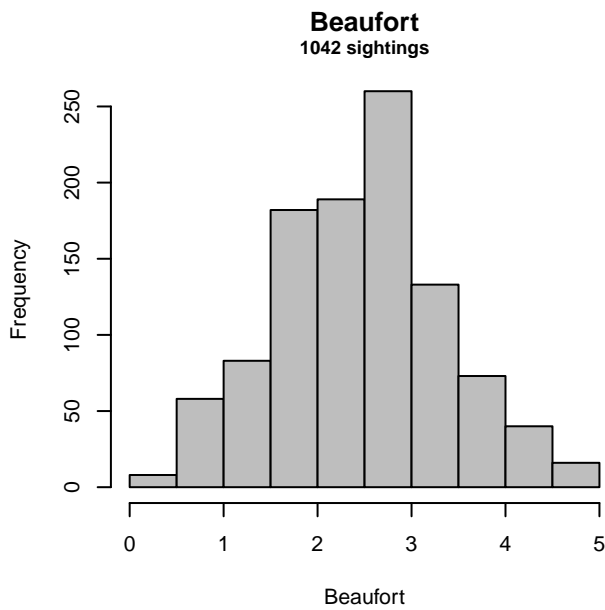


Figure 21: Distribution of the Beaufort covariate before (top row) and after (bottom row) observations were truncated to fit the NEFSC detection function.



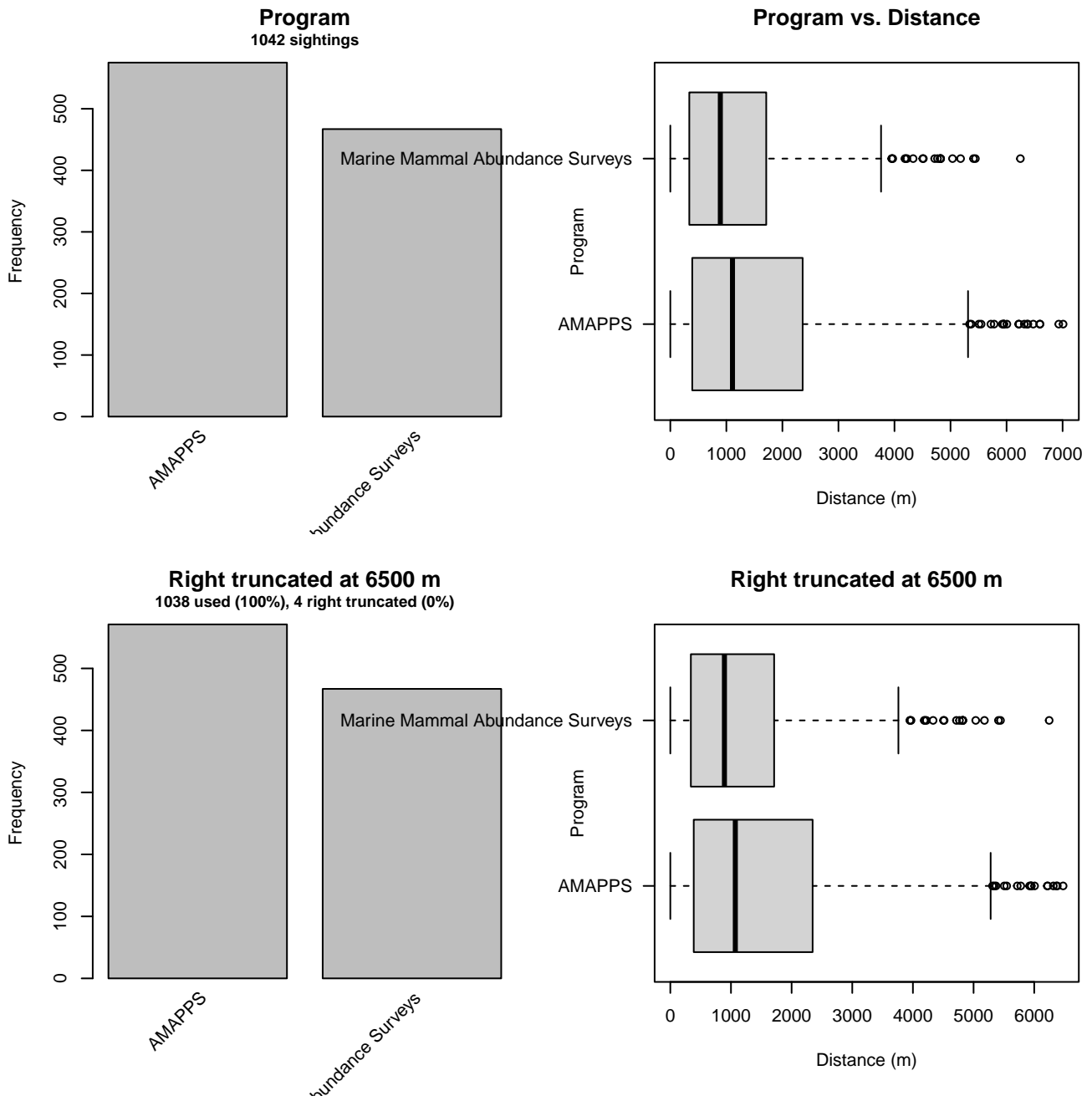


Figure 22: Distribution of the Program covariate before (top row) and after (bottom row) observations were truncated to fit the NEFSC detection function.

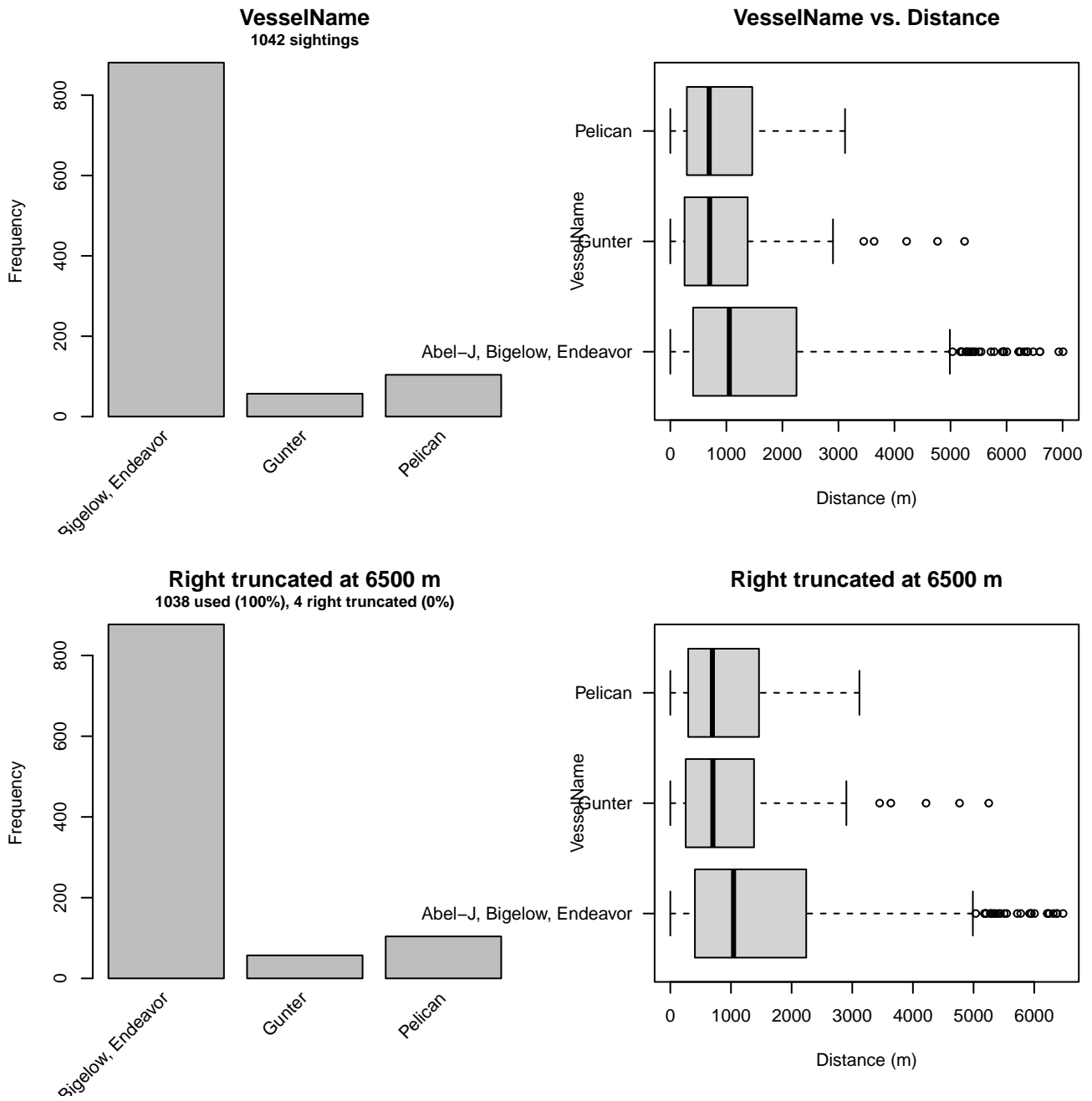


Figure 23: Distribution of the VesselName covariate before (top row) and after (bottom row) observations were truncated to fit the NEFSC detection function.

### 2.1.2.2 SEFSC

After right-truncating observations greater than 4500 m, we fitted the detection function to the 361 observations that remained (Table 13). The selected detection function (Figure 24) used a hazard rate key function with Beaufort (Figure 25) and VesselName (Figure 26) as covariates.

Table 13: Observations used to fit the SEFSC detection function.

ScientificName	n
Feresa attenuata/Peponocephala electra	7
Globicephala	227
Grampus griseus	121
Orcinus orca	1
Peponocephala electra	3
Pseudorca crassidens	2
<b>Total</b>	<b>361</b>

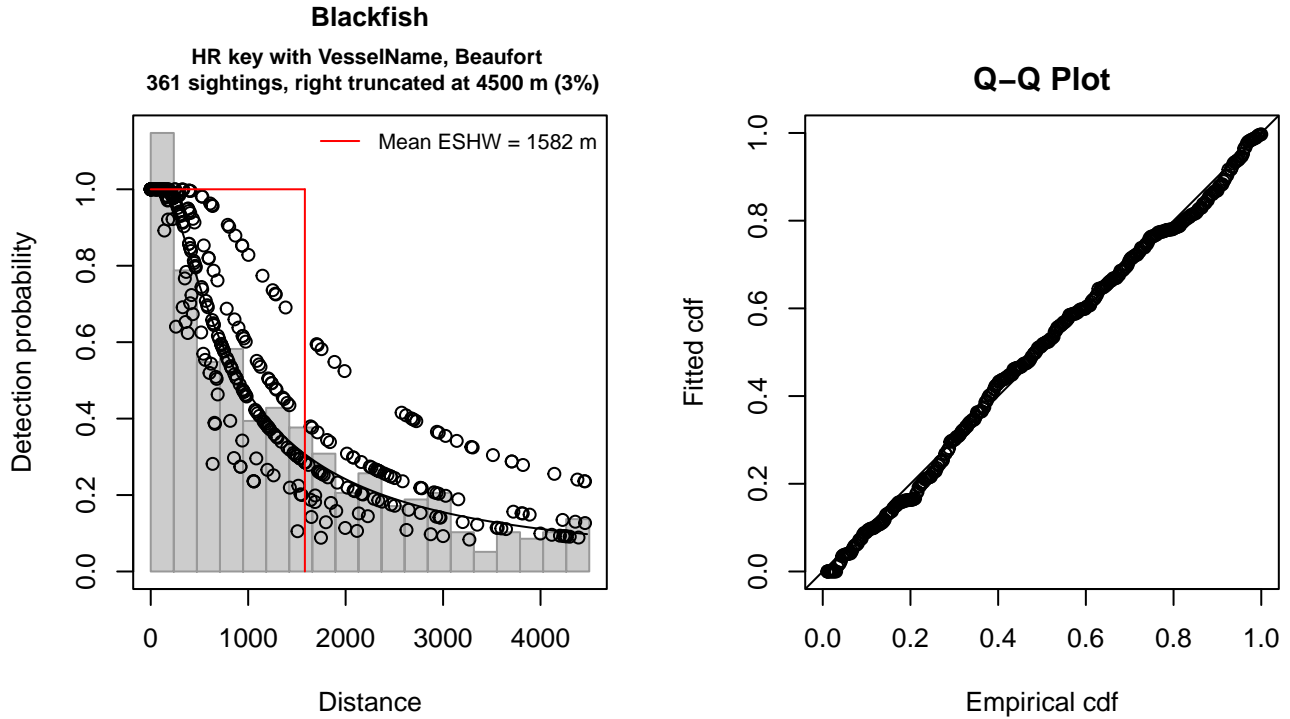


Figure 24: SEFSC detection function and Q-Q plot showing its goodness of fit.

Statistical output for this detection function:

Summary for ds object

Number of observations : 361  
 Distance range : 0 - 4500  
 AIC : 5876.279

Detection function:

Hazard-rate key function

Detection function parameters

Scale coefficient(s):

	estimate	se
(Intercept)	7.3597538	0.3426685
VesselNameOregon II	-0.5805409	0.4158932
Beaufort2	-0.5439643	0.4011114
Beaufort3-4	-0.8577400	0.3820711
Beaufort5	-1.2038982	0.5170081

Shape coefficient(s):

estimate se  
 (Intercept) 0.2309157 0.1254747

	Estimate	SE	CV
Average p	0.3253837	0.03477386	0.1068703
N in covered region	1109.4594048	128.24893603	0.1155959

Distance sampling Cramer-von Mises test (unweighted)  
 Test statistic = 0.112666 p = 0.526278

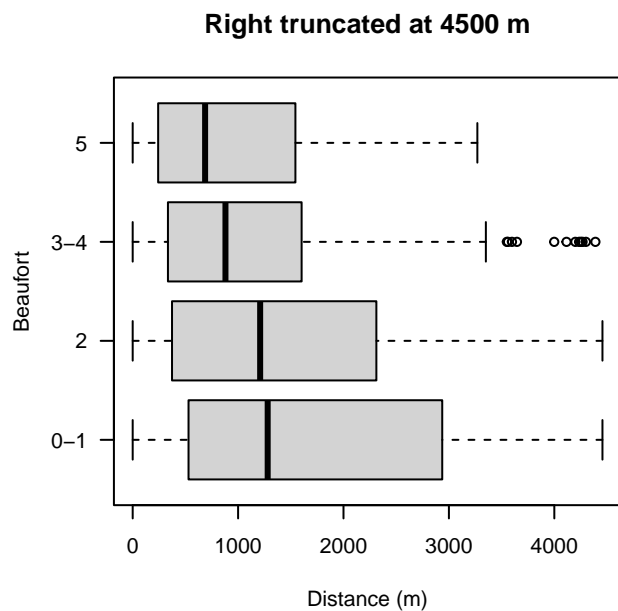
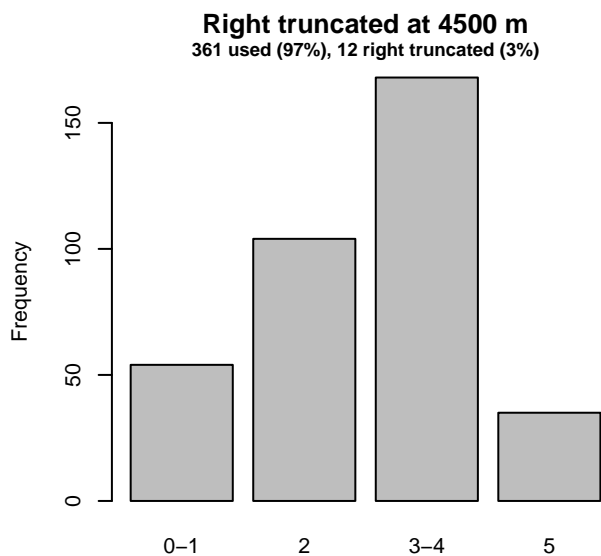
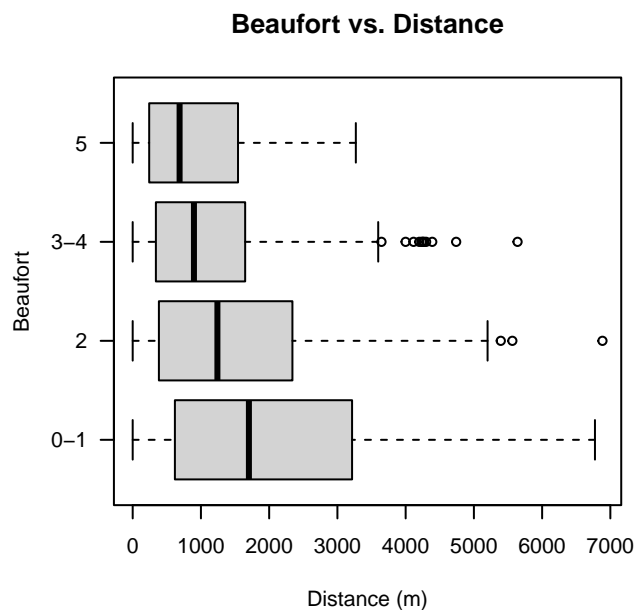
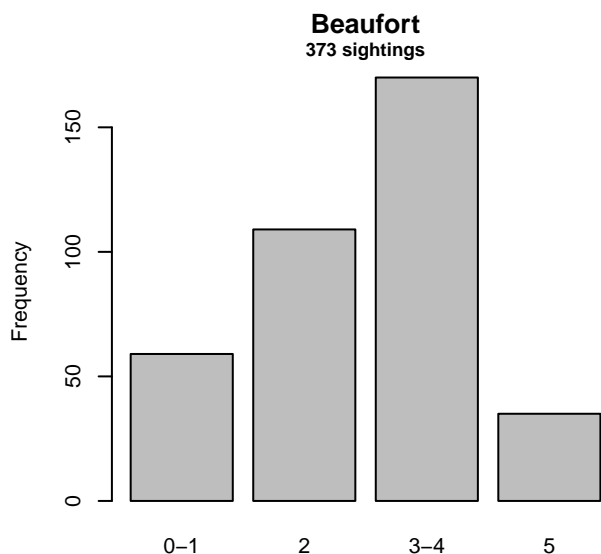


Figure 25: Distribution of the Beaufort covariate before (top row) and after (bottom row) observations were truncated to fit the SEFSC detection function.

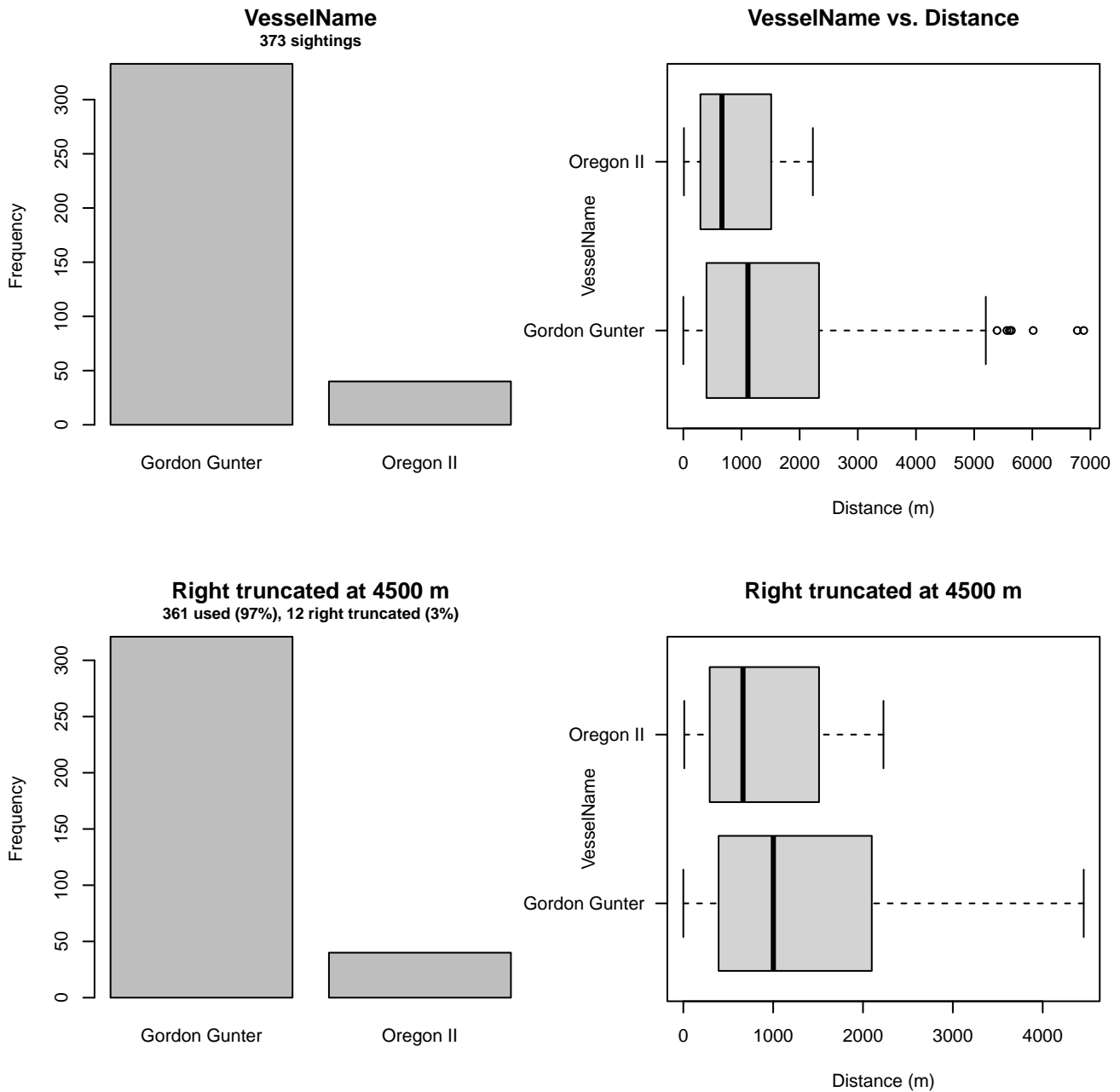


Figure 26: Distribution of the VesselName covariate before (top row) and after (bottom row) observations were truncated to fit the SEFSC detection function.

### 2.1.2.3 Song of the Whale

After right-truncating observations greater than 1500 m, we fitted the detection function to the 86 observations that remained (Table 14). The selected detection function (Figure 27) used a hazard rate key function with Beaufort (Figure 28) and Clouds (Figure 29) as covariates.

Table 14: Observations used to fit the Song of the Whale detection function.

ScientificName	n
Globicephala	48
Globicephala macrorhynchus	10
Globicephala melas	3
Grampus griseus	15
Orcinus orca	6
Pseudorca crassidens	4
<b>Total</b>	<b>86</b>

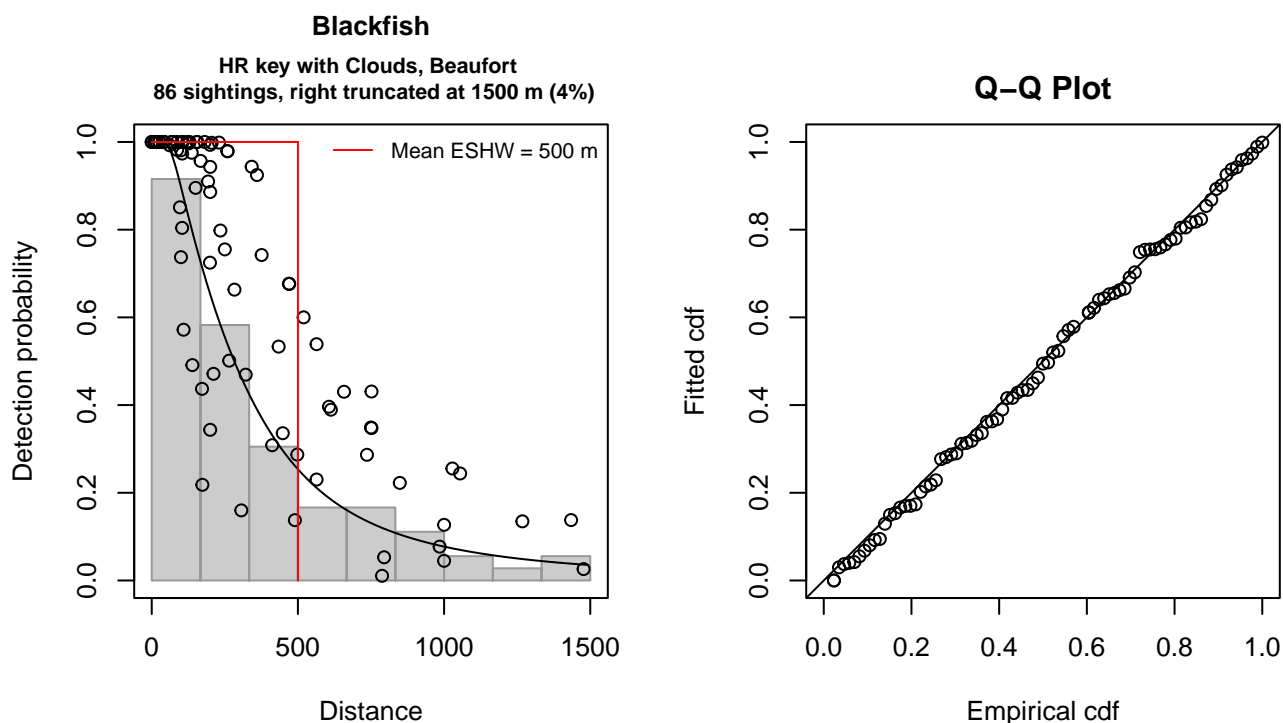


Figure 27: Song of the Whale detection function and Q-Q plot showing its goodness of fit.

Statistical output for this detection function:

Summary for ds object

Number of observations : 86  
 Distance range : 0 - 1500  
 AIC : 1170.598

Detection function:

Hazard-rate key function

Detection function parameters

Scale coefficient(s):

	estimate	se
(Intercept)	6.4796997	0.26905817
Clouds	-0.1344265	0.04822789
Beaufort3-4	-0.6588095	0.31406041

Shape coefficient(s):

	estimate	se
(Intercept)	0.7265327	0.1798353

	Estimate	SE	CV
Average p	0.265116	0.04508089	0.1700421
N in covered region	324.386340	63.44454836	0.1955833

Distance sampling Cramer-von Mises test (unweighted)  
 Test statistic = 0.019751 p = 0.997226

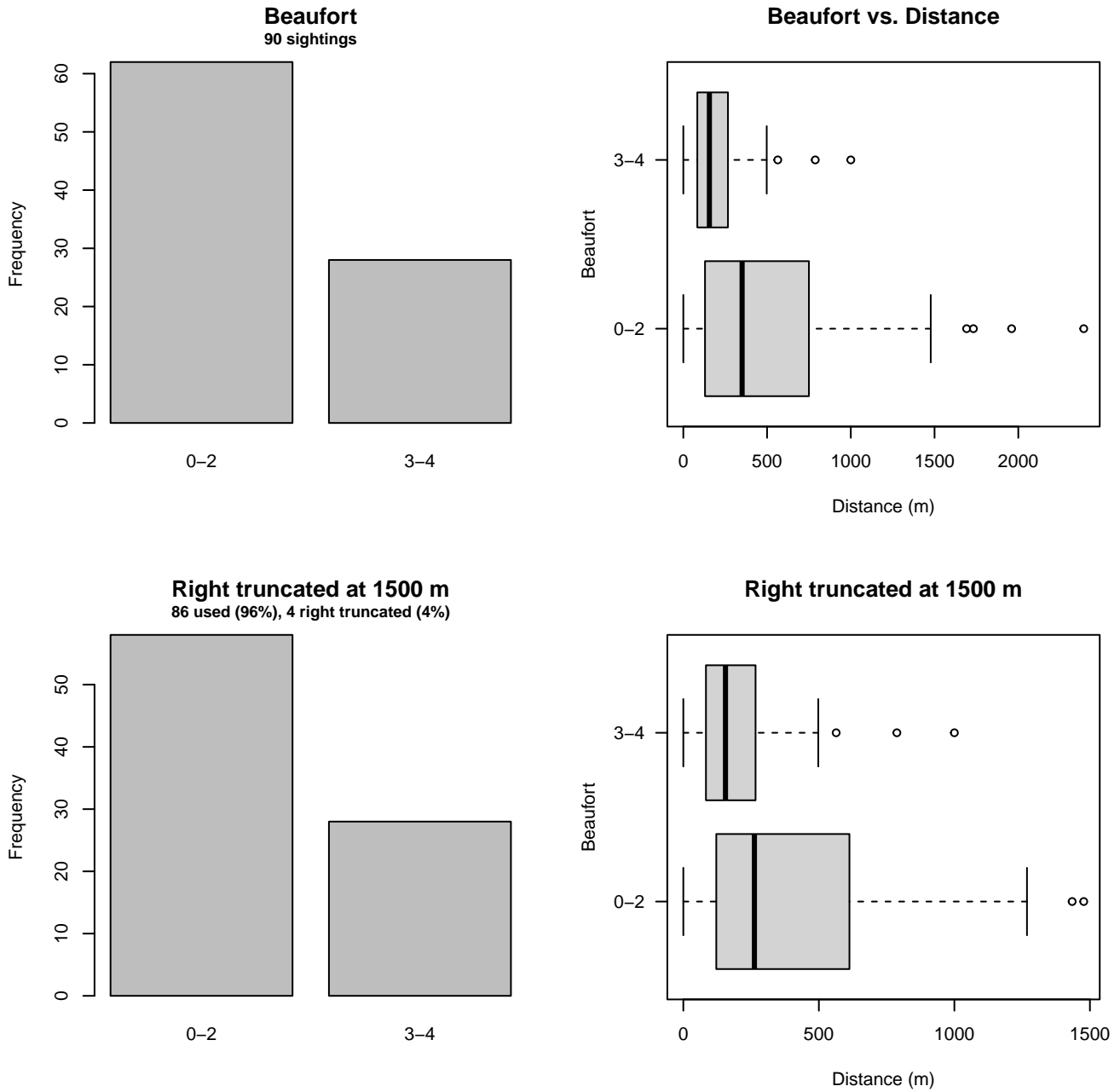


Figure 28: Distribution of the Beaufort covariate before (top row) and after (bottom row) observations were truncated to fit the Song of the Whale detection function.

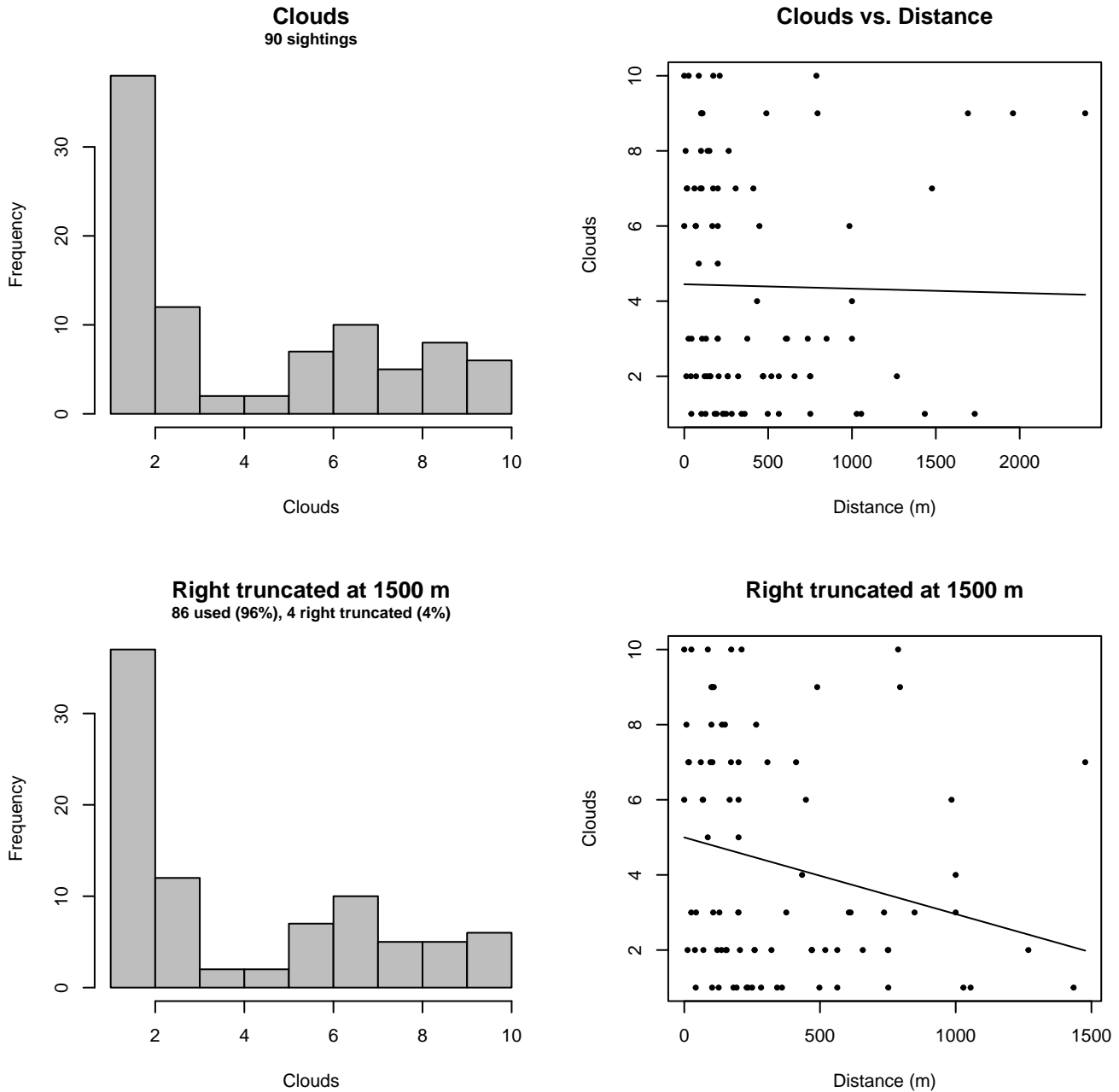


Figure 29: Distribution of the Clouds covariate before (top row) and after (bottom row) observations were truncated to fit the Song of the Whale detection function.

### 3 Bias Corrections

Density surface modeling methodology uses *distance sampling* (Buckland et al. 2001) to model the probability that an observer on a line transect survey will detect an animal given the perpendicular distance to it from the transect line. Distance sampling assumes that detection probability is 1 when perpendicular distance is 0. When this assumption is not met, detection probability is biased high, leading to an underestimation of density and abundance. This is known as the  $g_0 < 1$  problem, where  $g_0$  refers to the detection probability at distance 0. Modelers often try to address this problem by estimating  $g_0$  empirically and dividing it into estimated density or abundance, thereby correcting those estimates to account for the animals that were presumed missed.

Two important sources of bias for visual surveys are known as *availability bias*, in which an animal was present on the transect line but impossible to detect, e.g. because it was under water, and *perception bias*, in which an animal was present and available but not noticed, e.g. because of its small size or cryptic coloration or behavior (Marsh and Sinclair 1989). Modelers often



estimate the influence of these two sources of bias on detection probability independently, yielding two estimates of  $g_0$ , hereafter referred to as  $g_{0A}$  and  $g_{0P}$ , and multiply them together to obtain a final, combined estimate:  $g_0 = g_{0A} \cdot g_{0P}$ .

Our overall approach was to perform this correction on a per-observation basis, to have the flexibility to account for many factors such as platform type, surveyor institution, group size, group composition (e.g. singleton, mother-calf pair, or surface active group), and geographic location (e.g. feeding grounds vs. calving grounds). The level of complexity of the corrections varied by species according to the amount of information available, with North Atlantic right whale having the most elaborate corrections, derived from a substantial set of publications documenting its behavior, and various lesser known odontocetes having corrections based only on platform type (aerial or shipboard), derived from comparatively sparse information. Here we document the corrections used for false killer whale.

### 3.1 Aerial Surveys

The only false killer whale sighting that was reported across all aerial surveys contributed by the collaborators was from NOAA SEFSC’s summer 2016 aerial survey, off Maryland, just east of the shelf break, between Baltimore and Wilmington Canyons. This sighting was left-truncated during detection modeling (see Section 2.1.1.3) so it was not available for subsequent density modeling. Thus, with no aerial sightings, no aerial bias corrections were necessary under our methodology.

### 3.2 Shipboard Surveys

Most of the shipboard surveys in our analysis used high-power (25x150), pedestal-mounted binoculars. Garrison et al. (in prep.) developed perception bias corrections using two team, MRDS methodology (Burt et al. 2014) for high-power binocular surveys conducted in 2003-2018 by SEFSC during the Gulf of Mexico Marine Assessment Program for Protected Species (GoMMAPPS) and predecessor campaigns. We favored this estimate slightly over a similar effort by Palka et al. (2021) who developed estimates for the 2010-2017 AMAPPS program, because while both estimates were made for similar guilds of “blackfish” species, the latter was more heavily dominated by Risso’s dolphins and pilot whales. In any case, the estimates are similar:  $g_{0P} = 0.6415$  from Garrison et al. (in prep);  $g_{0P} = 0.71$  for SEFSC and  $g_{0P} = 0.50$  for NEFSC from Palka et al. (2021).

We applied Garrison’s estimate to all shipboard sightings, including one made during MCR’s 2019 Song of the Whale survey, which searched by naked eye, as we were not able to locate a suitable correction factor for this species for naked eye surveys. For all surveys, to account for the influence of large group sizes on perception bias, we followed Barlow and Forney (2007) and set the perception bias correction factor for sightings of more than 20 animals to  $g_{0P} = 0.97$ . Given that the dive interval of this species (Minamikawa et al. (2013); Table 15) was short relative to the amount of time a given patch of water remained in view to shipboard observers, we assumed that no availability bias correction was needed ( $g_{0A} = 1$ ).

Table 15: Surface and dive intervals for false killer whale used to estimate availability bias corrections.

Surface Interval (s)	Dive Interval (s)	Source
131.5	313	Minamikawa et al. (2013)

Table 16: Perception and availability bias corrections for false killer whale applied to shipboard surveys.

Surveys	Searching Method	Group Size	$g_{0P}$	$g_{0P}$ Source	$g_{0A}$	$g_{0A}$ Source
All	All	$\leq 20$	0.6415	Garrison et al. (in prep.)	1	Assumed
All	All	$> 20$	0.9700	Barlow and Forney (2007)	1	Assumed

## 4 Geographic Strata

With so few sightings, it was not possible to fit a traditional density surface model that related density observed on survey segments to environmental covariates. Nor was it possible to make proper design-based abundance estimates using traditional distance sampling (Buckland et al. 2001), because the aggregate surveys provided very heterogeneous coverage that did not together constitute a proper systematic survey design.

To provide interested parties with at least rough estimates of density in ecologically relevant geographic strata, we first split the study area into five strata (Figure 1) at major habitat boundaries. We placed our first split at the continental shelf break,

defined as the 100 meter isobath, separating the study area in into shelf and offshore regions. (We manually cut across the Northeast Channel of the Gulf of Maine, so that the Gulf was considered part of the shelf.) We then split the shelf region at Cape Hatteras, a location where the Gulf Stream separates from the continental shelf, which has previously been used to delineate community structure in marine mammals (Schick et al. 2011). We also split the shelf region at the Nantucket Shoals, which separate the Gulf of Maine from the New York Bight. We split off the bays and sounds of New York, Rhode Island, and southern Massachusetts, generally at the 10 m isobath, on the basis that these inshore areas are rarely visited by cetaceans of any species. Finally, we split the offshore region at the north wall of the Gulf Stream, starting at Cape Hatteras and extending along the north wall of the Gulf Stream, as defined with a long-term climatology of total kinetic energy, to the edge of the study area.

We then derived density estimates for each stratum by fitting a model with no covariates, under the assumption that density would be distributed uniformly within the stratum. This assumption, if true, would mean we would obtain similar density estimates for a given stratum under any sampling design, and therefore it would not matter if there was some heterogeneity in sampling within the stratum. However, we strongly caution that this assumption did not hold for the other, more-common species we successfully modeled with traditional density surface modeling, as evidenced by the non-uniform patterns in density predicted by those species' models. That said, when those results are viewed at a very coarse, ecoregional scale, the boundaries used here often correlate with boundaries or strong gradients in density in those models. Thus, for the much rarer species, such as false killer whale documented here, we offer this simplified approach as a rough-and-ready substitute for a full density surface model.

In this section, we present maps of each stratum that contained sightings, with tallies of effort and sightings that occurred.

#### 4.1 Offshore North of Gulf Stream

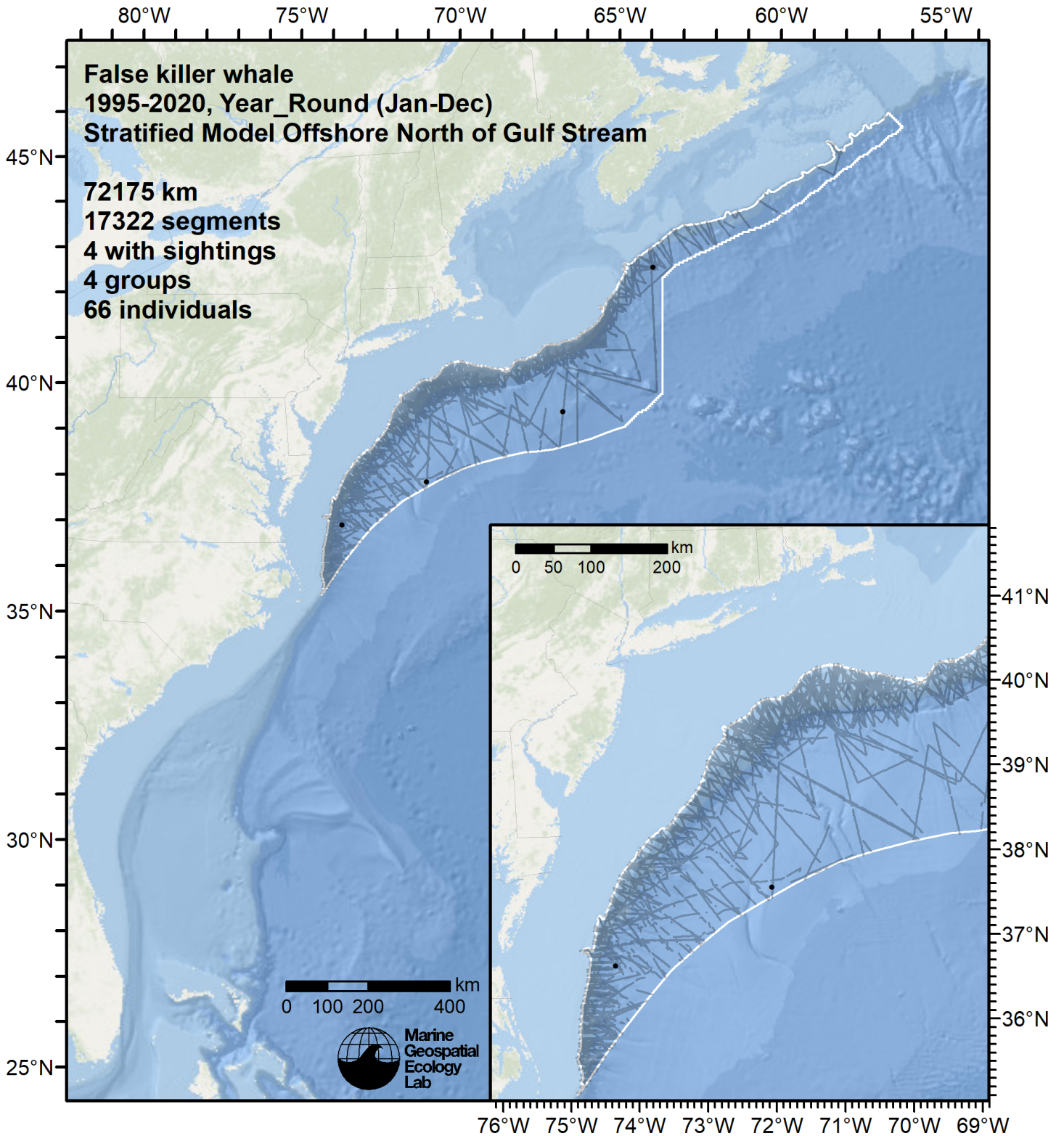


Figure 30: Survey segments and sightings used to estimate false killer whale density for the "Offshore North of Gulf Stream" region. Black points indicate segments with observations.



## 4.2 Offshore Gulf Stream and South

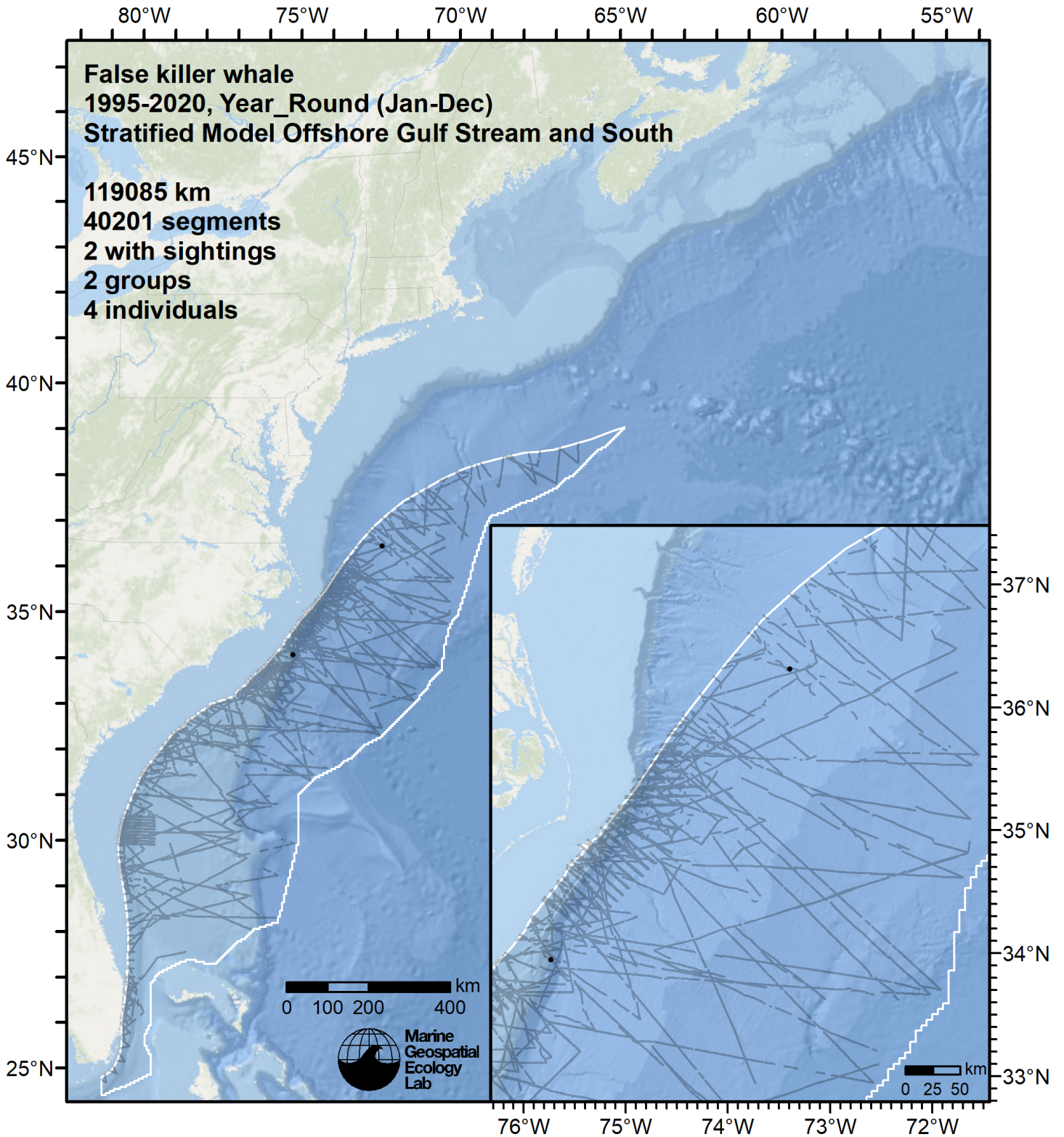


Figure 31: Survey segments and sightings used to estimate false killer whale density for the "Offshore Gulf Stream and South" region. Black points indicate segments with observations.

## 5 Predictions

### 5.1 Summarized Predictions

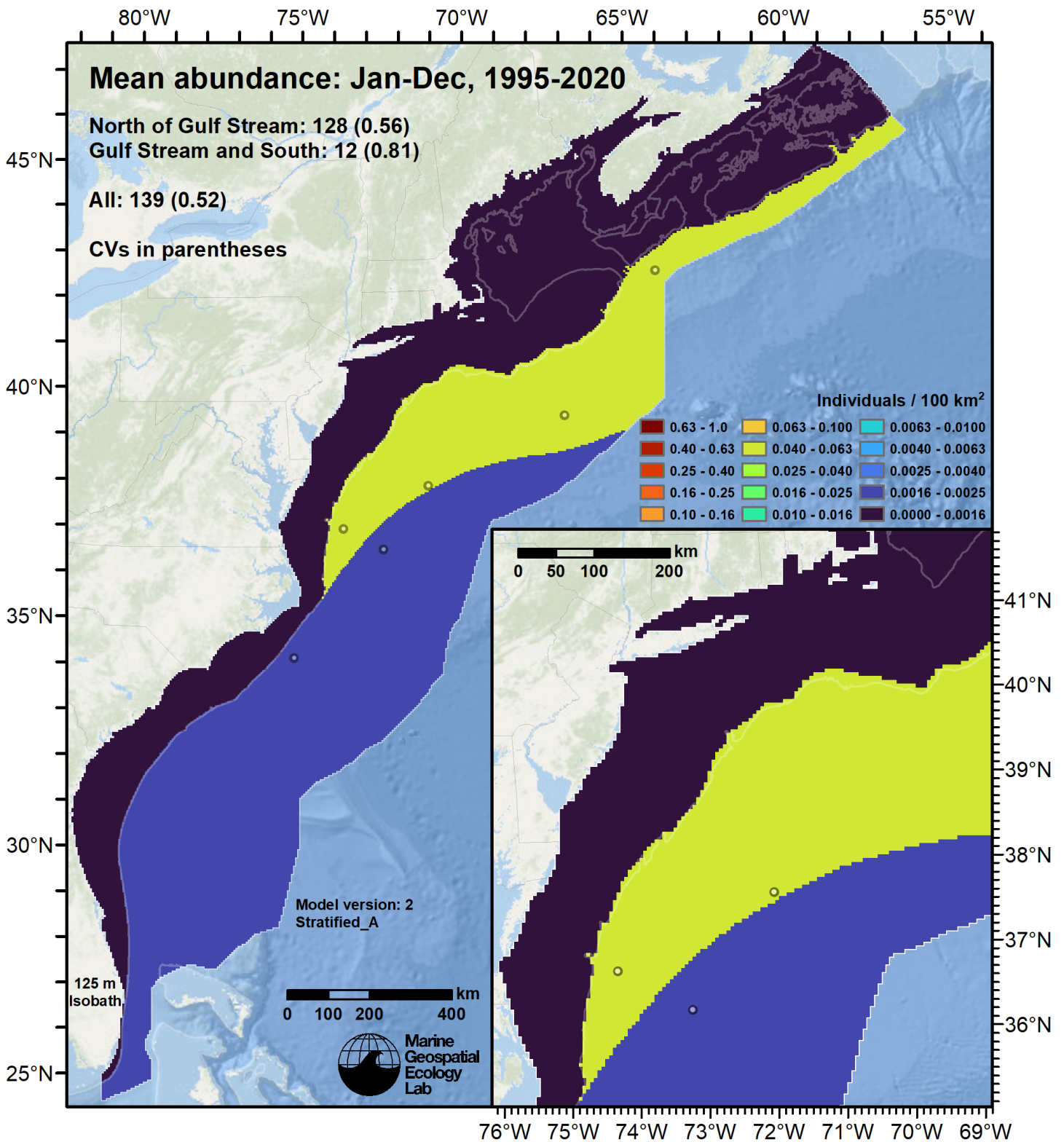


Figure 32: False killer whale density estimated for the indicated period. Open circles indicate segments with observations. The abundance estimate and its coefficient of variation (CV) are given in the subtitle.



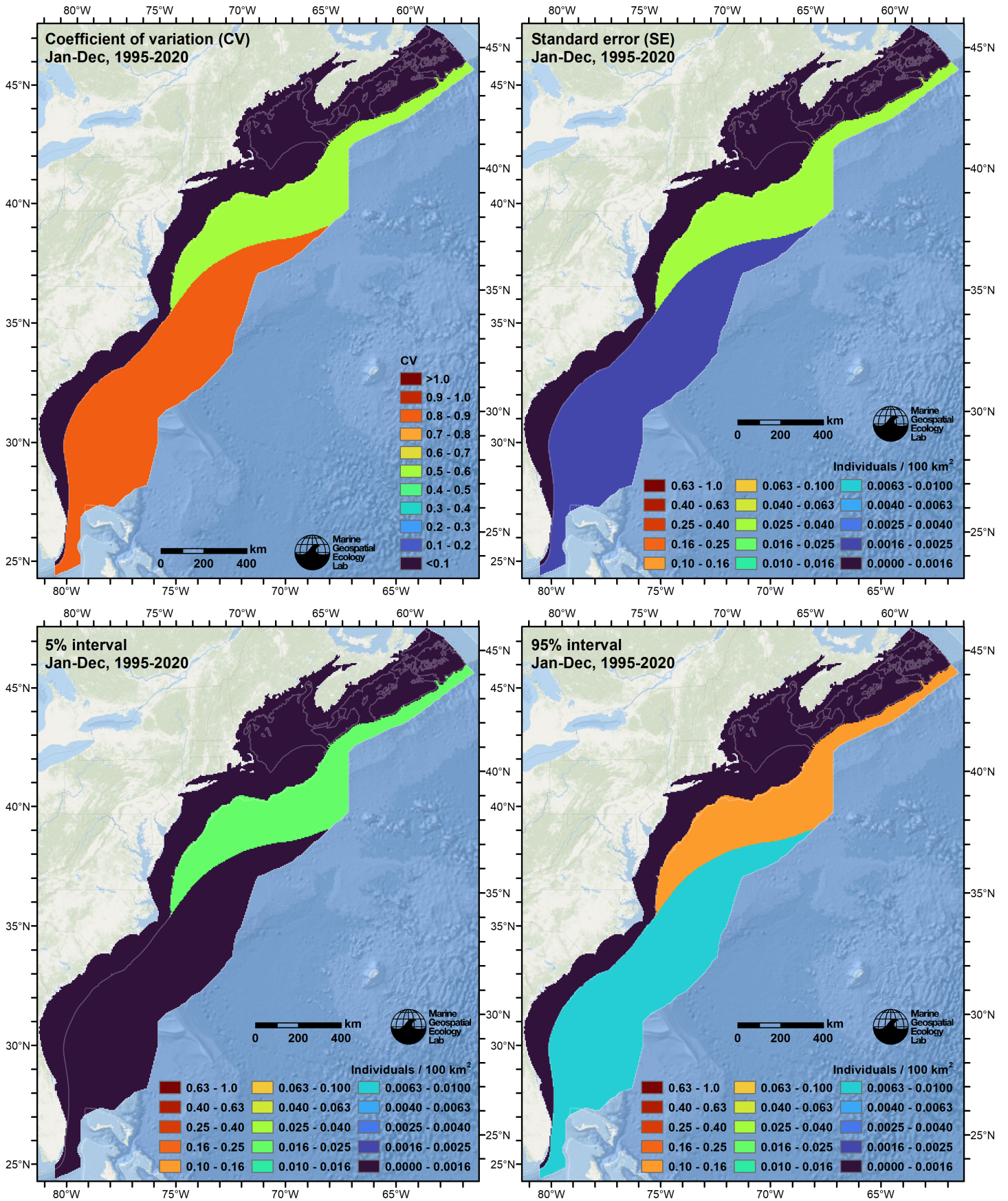


Figure 33: Uncertainty statistics for the false killer whale estimated density surface (Figure 32).

Table 17: False killer whale abundance and density estimated for each stratum.

Region	Abundance	CV	95% Interval	Area (km <sup>2</sup> )	Density (indiv. / 100 km <sup>2</sup> )
Offshore Gulf Stream and South	12	0.814	3 - 48	499,300	0.0024
Offshore North of Gulf Stream	128	0.562	46 - 356	253,575	0.0503
Shelf Cape Hatt. to Nant. Shoals	0	0.000	0 - 0	104,425	0.0000
Shelf North of Nantucket Shoals	0	0.000	0 - 0	302,025	0.0000
Shelf South of Cape Hatteras	0	0.000	0 - 0	105,500	0.0000
Sounds of NY, RI, and MA	0	0.000	0 - 0	8,600	0.0000
Total	139	0.519	54 - 363	1,273,425	0.0109

## 5.2 Abundance Comparisons

### 5.2.1 NOAA Stock Assessment Report

Table 18: Comparison of regional abundance estimates from the 2019 NOAA Stock Assessment Report (SAR) (Hayes et al. (2020)) to estimates from this density model extracted from roughly comparable zones (Figure 34 below). The SAR estimates were based on a single year of surveying, while the model estimates were taken from the multi-year mean density surface we provide to model users (Section 5.1).

2019 Stock Assessment Report			Density Model		
Month/Year	Area	$N_{est}$	Period	Zone	Abundance
Jun-Aug 2011	Central Virginia to lower Bay of Fundy	0			
Jun-Aug 2011	Central Florida to central Virginia	442			
Jun-Aug 2011	Total	442			
Jun-Aug 2016	New Jersey to lower Bay of Fundy <sup>a</sup>	1,182	Jan-Dec 1995-2020	NEFSC	96
Jun-Aug 2016	Central Florida to New Jersey <sup>b</sup>	609	Jan-Dec 1995-2020	SEFSC	21
			Jan-Dec 1995-2020	Canada <sup>c</sup>	21
Jun-Aug 2016	Total	1,791	Jan-Dec 1995-2020	Total	138

<sup>a</sup> Estimate originally from Palka (2020).

<sup>b</sup> Estimate originally from Garrison (2020).

<sup>c</sup> The SAR did not provide an estimate for this area. DFO's 2007 and 2016 surveys of the area did not report any sightings (Lawson and Gosselin (2018)).

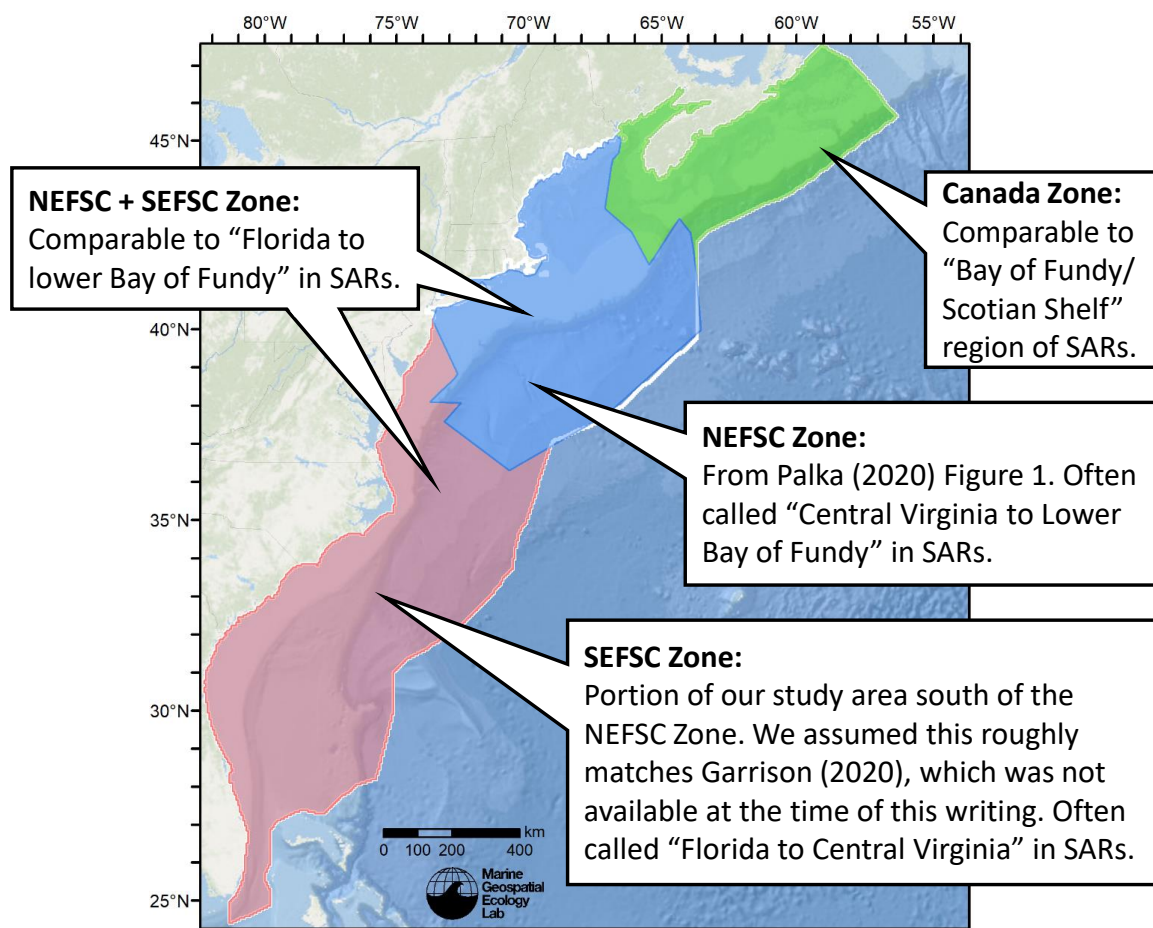


Figure 34: Zones for which we extracted abundance estimates from the density model for comparison to estimates from the NOAA Stock Assessment Report.



## 5.2.2 Previous Density Model

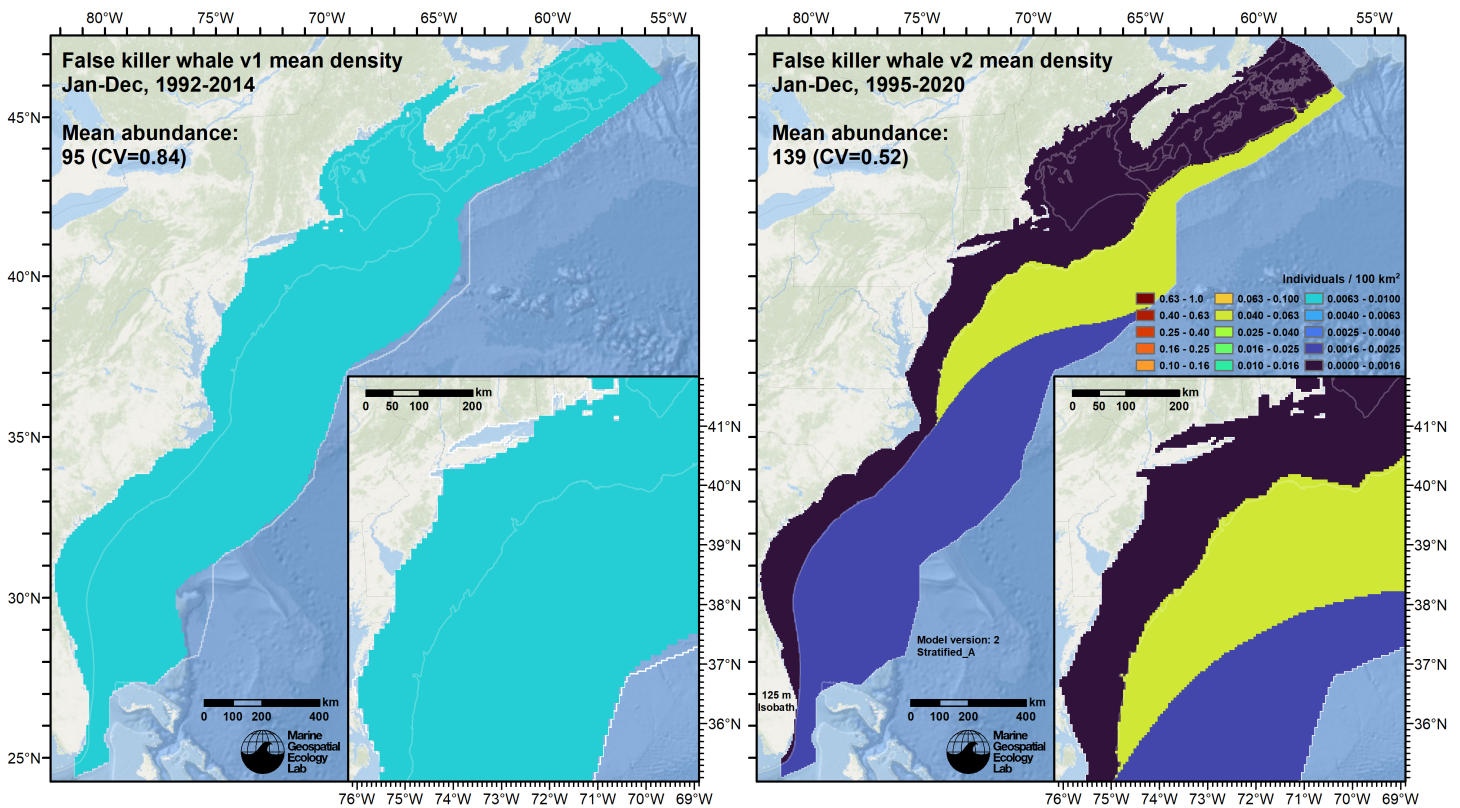


Figure 35: Comparison of the mean density predictions from the previous model (left) released by Roberts et al. (2016) to those from this model (right).

## 6 Discussion

False killer whales are found in all tropical and warm temperate oceans, and occasionally in cold temperate waters; they appear to be naturally uncommon throughout their range (Baird 2009). They are typically characterized as a pelagic species but are known to utilize shallow waters around oceanic islands and occasionally continental shelves (Baird 2009, 2018). In the eastern Atlantic they have been recorded as far north as Norway (Leatherwood et al. 1989). Sightings have been uncommon in the western North Atlantic but the species is believed to occur routinely, based on sighting, stranding, and bycatch records (Hayes et al. 2020).

In our east coast study area, the collaborators only reported six on-effort sightings over the analyzed period of 1995-2020 (a seventh was left-truncated; see Section 3). With insufficient sightings to model density from environmental predictors, we estimated density in five geographic strata with a simplified approach (Section 4). All of the sightings occurred in the two offshore strata, yielding a total abundance estimate of 139. The NOAA Stock Assessment Reports previously estimated abundance at 442 during the 2011 AMAPPS campaign and 1,791 during the 2016 AMAPPS campaign (Table 18). While NOAA's estimates are much higher than ours, we note that they did not sight any false killer whales on their two prior broad scale campaigns, in 2004 and 1998, meaning that abundance was effectively zero under the Stock Assessment process during those earlier years. NOAA did make a couple of sightings on smaller surveys during the analyzed period (in 1995 and 2006). We presume these earlier sightings did not result in formal abundance estimates because the surveys were not sufficiently broad scale. Given that we included all of NOAA's surveys back to 1995, not just those in 2011 and 2016, we are not surprised that our multi-year estimate is lower than NOAA's for those two years referenced in the SAR. We considered dropping the earlier years from our estimate, on the basis that the population could be growing, and perhaps base it on surveys from 2011 and later. While population growth cannot be ruled out, we agree with the SAR's assessment that the encounter rate is too low to assess or interpret trends in population size, and we therefore judged it best to include the earlier years. Finally, we must reiterate that our stratified modeling approach does not fully correct for the heterogeneous distribution of sampling effort in space in time, which could have biased our abundance estimate (see Section 4).

In our prior model, we considered the entire study area to be a single stratum (Figure 35), on the basis that the species does occasionally occur over the continental shelf. Evidence of this for our study area can be seen in the OBIS-SEAMAP

system (Halpin et al. 2009), which contains additional sightings not utilizable in our model. These included a sighting south of Isle Au Haut, Maine reported by a NOAA shipboard abundance survey in August 1995 (this survey was not used in our models because NOAA no longer had the original sighting distances for this old survey). Another notable shipboard sighting was made in Cape Cod Bay in 1978 by a University of Rhode Island research team. Finally, eight sightings were reported near Montauk, NY between 1990-1993 by commercial whale watching vessels. Our approach for the 2022 modeling cycle was to split the study area into five geographic strata based on major habitat boundaries (see Section 4), and then estimate abundance within each. Because we had no sightings over the four shelf strata, our new model estimates zero abundance there, and abundance in the offshore strata is substantially higher. We caution that the opportunistic sightings referenced above confirm that false killer whales very occasionally occur in the shelf strata. Should an on-effort sighting be reported in the future by a collaborator, the model can be updated to account for it.

## References

- Baird RW (2009) [False Killer Whale](#). In: Encyclopedia of Marine Mammals, 2nd ed. Elsevier, pp 405–406
- Baird RW (2018) [False Killer Whale](#). In: Encyclopedia of Marine Mammals, 3rd ed. Elsevier, pp 347–349
- Barco SG, Burt L, DePerte A, Digiovanni R Jr. (2015) Marine Mammal and Sea Turtle Sightings in the Vicinity of the Maryland Wind Energy Area July 2013-June 2015, VAQF Scientific Report #2015-06. Virginia Aquarium & Marine Science Center Foundation, Virginia Beach, VA
- Barlow J, Forney KA (2007) [Abundance and population density of cetaceans in the California Current ecosystem](#). Fishery Bulletin 105:509–526.
- Blaylock RA, Hoggard W (1994) [Preliminary Estimates of Bottlenose Dolphin Abundance in Southern U.S. Atlantic and Gulf of Mexico Continental Shelf Waters: NOAA Technical Memorandum NMFS-SEFSC-356](#). NOAA National Marine Fisheries Service, Southeast Fisheries Science Center, Miami, FL
- Buckland ST, Anderson DR, Burnham KP, Laake JL, Borchers DL, Thomas L (2001) Introduction to Distance Sampling: Estimating Abundance of Biological Populations. Oxford University Press, Oxford, UK
- Burt ML, Borchers DL, Jenkins KJ, Marques TA (2014) Using mark-recapture distance sampling methods on line transect surveys. *Methods in Ecology and Evolution* 5:1180–1191. doi: [10.1111/2041-210X.12294](#)
- Cole T, Gerrior P, Merrick RL (2007) [Methodologies of the NOAA National Marine Fisheries Service Aerial Survey Program for Right Whales \(\*Eubalaena glacialis\*\) in the Northeast U.S., 1998-2006](#). U.S. Department of Commerce, Woods Hole, MA
- Cotter MP (2019) Aerial Surveys for Protected Marine Species in the Norfolk Canyon Region: 2018–2019 Final Report. HDR, Inc., Virginia Beach, VA
- Foley HJ, Paxton CGM, McAlarney RJ, Pabst DA, Read AJ (2019) Occurrence, Distribution, and Density of Protected Species in the Jacksonville, Florida, Atlantic Fleet Training and Testing (AFTT) Study Area. Duke University Marine Lab, Beaufort, NC
- Garrison LP (2020) [Abundance of cetaceans along the southeast U.S. East coast from a summer 2016 vessel survey. PRD Contribution # PRD-2020-04](#). NOAA National Marine Fisheries Service, Southeast Fisheries Science Center, Miami, FL
- Garrison LP, Martinez A, Maze-Foley K (2010) [Habitat and abundance of cetaceans in Atlantic Ocean continental slope waters off the eastern USA](#). *Journal of Cetacean Research and Management* 11:267–277.
- Geo-Marine, Inc. (2010) [New Jersey Department of Environmental Protection Baseline Studies Final Report Volume III: Marine Mammal and Sea Turtle Studies](#). Geo-Marine, Inc., Plano, TX
- Halpin P, Read A, Fujioka E, Best B, Donnelly B, Hazen L, Kot C, Urian K, LaBrecque E, Dimatteo A, Cleary J, Good C, Crowder L, Hyrenbach KD (2009) OBIS-SEAMAP: The World Data Center for Marine Mammal, Sea Bird, and Sea Turtle Distributions. *Oceanography* 22:104–115. doi: [10.5670/oceanog.2009.42](#)
- Hayes SA, Josephson E, Maze-Foley K, Rosel PE, Byrd B, Chavez-Rosales S, Cole TV, Garrison LP, Hatch J, Henry A, Horstman SC, Litz J, Lyssikatos MC, Mullin KD, Orphanides C, Pace RM, Palka DL, Powell J, Wenzel FW (2020) [US Atlantic and Gulf of Mexico Marine Mammal Stock Assessments - 2019](#). NOAA National Marine Fisheries Service, Northeast Fisheries Science Center, Woods Hole, MA
- Lawson JW, Gosselin J-F (2018) Estimates of cetacean abundance from the 2016 NAISS aerial surveys of eastern Canadian waters, with a comparison to estimates from the 2007 TNASS. NAMMCO SC/25/AE/09. In: Proceedings of the NAMMCO 25th Scientific Committee (SC). North Atlantic Marine Mammal Commission, Bergen-Tromsø, Norway,

- Leatherwood S, McDonald D, Baird RW, Scott MD (1989) [The false killer whale, \*Pseudorca crassidens\* \(OWEN, 1846\): A summary of information available through 1988.](#)
- Leiter S, Stone K, Thompson J, Accardo C, Wikgren B, Zani M, Cole T, Kenney R, Mayo C, Kraus S (2017) North Atlantic right whale *Eubalaena glacialis* occurrence in offshore wind energy areas near Massachusetts and Rhode Island, USA. *Endang Species Res* 34:45–59. doi: [10.3354/esr00827](#)
- Mallette SD, Lockhart GG, McAlarney RJ, Cummings EW, McLellan WA, Pabst DA, Barco SG (2014) Documenting Whale Migration off Virginia’s Coast for Use in Marine Spatial Planning: Aerial and Vessel Surveys in the Proximity of the Virginia Wind Energy Area (VA WEA), VAQF Scientific Report 2014-08. Virginia Aquarium & Marine Science Center Foundation, Virginia Beach, VA
- Mallette SD, Lockhart GG, McAlarney RJ, Cummings EW, McLellan WA, Pabst DA, Barco SG (2015) Documenting Whale Migration off Virginia’s Coast for Use in Marine Spatial Planning: Aerial Surveys in the Proximity of the Virginia Wind Energy Area (VA WEA) Survey/Reporting Period: May 2014 - December 2014, VAQF Scientific Report 2015-02. Virginia Aquarium & Marine Science Center Foundation, Virginia Beach, VA
- Mallette SD, McAlarney RJ, Lockhart GG, Cummings EW, Pabst DA, McLellan WA, Barco SG (2017) [Aerial Survey Baseline Monitoring in the Continental Shelf Region of the VACAPES OPAREA: 2016 Annual Progress Report.](#) Virginia Aquarium & Marine Science Center Foundation, Virginia Beach, VA
- Marsh H, Sinclair DF (1989) Correcting for Visibility Bias in Strip Transect Aerial Surveys of Aquatic Fauna. *The Journal of Wildlife Management* 53:1017. doi: [10.2307/3809604](#)
- McAlarney R, Cummings E, McLellan W, Pabst A (2018) Aerial Surveys for Protected Marine Species in the Norfolk Canyon Region: 2017 Annual Progress Report. University of North Carolina Wilmington, Wilmington, NC
- McLellan WA, McAlarney RJ, Cummings EW, Read AJ, Paxton CGM, Bell JT, Pabst DA (2018) Distribution and abundance of beaked whales (Family Ziphiidae) Off Cape Hatteras, North Carolina, U.S.A. *Marine Mammal Science*. doi: [10.1111/mms.12500](#)
- Minamikawa S, Watanabe H, Iwasaki T (2013) Diving behavior of a false killer whale, *Pseudorca crassidens*, in the Kuroshio–Oyashio transition region and the Kuroshio front region of the western North Pacific. *Marine Mammal Science* 29:177–185. doi: [10.1111/j.1748-7692.2011.00532.x](#)
- Mullin KD, Fulling GL (2003) [Abundance of cetaceans in the southern U.S. North Atlantic Ocean during summer 1998.](#) *Fishery Bulletin* 101:603–613.
- O’Brien O, Pendleton DE, Ganley LC, McKenna KR, Kenney RD, Quintana-Rizzo E, Mayo CA, Kraus SD, Redfern JV (2022) Repatriation of a historical North Atlantic right whale habitat during an era of rapid climate change. *Sci Rep* 12:12407. doi: [10.1038/s41598-022-16200-8](#)
- Palka D (2020) [Cetacean Abundance in the US Northwestern Atlantic Ocean Summer 2016.](#) *Northeast Fish Sci Cent Ref Doc. 20-05.* NOAA National Marine Fisheries Service, Northeast Fisheries Science Center, Woods Hole, MA
- Palka D, Aichinger Dias L, Broughton E, Chavez-Rosales S, Cholewiak D, Davis G, DeAngelis A, Garrison L, Haas H, Hatch J, Hyde K, Jech M, Josephson E, Mueller-Brennan L, Orphanides C, Pegg N, Sasso C, Sigourney D, Soldevilla M, Walsh H (2021) [Atlantic Marine Assessment Program for Protected Species: FY15 – FY19 \(OCS Study BOEM 2021-051\).](#) U.S. Department of the Interior, Bureau of Ocean Energy Management, Washington, DC
- Palka DL (2006) [Summer abundance estimates of cetaceans in US North Atlantic navy operating areas \(NEFSC Reference Document 06-03\).](#) U.S. Department of Commerce, Northeast Fisheries Science Center, Woods Hole, MA
- Palka DL, Chavez-Rosales S, Josephson E, Cholewiak D, Haas HL, Garrison L, Jones M, Sigourney D, Waring G, Jech M, Broughton E, Soldevilla M, Davis G, DeAngelis A, Sasso CR, Winton MV, Smolowitz RJ, Fay G, LaBrecque E, Leiness JB, Dettloff K, Warden M, Murray K, Orphanides C (2017) [Atlantic Marine Assessment Program for Protected Species: 2010-2014 \(OCS Study BOEM 2017-071\).](#) U.S. Department of the Interior, Bureau of Ocean Energy Management, Washington, DC
- Quintana-Rizzo E, Leiter S, Cole T, Hagbloom M, Knowlton A, Nagelkirk P, O’Brien O, Khan C, Henry A, Duley P, Crowe L, Mayo C, Kraus S (2021) Residency, demographics, and movement patterns of North Atlantic right whales *Eubalaena glacialis* in an offshore wind energy development area in southern New England, USA. *Endang Species Res* 45:251–268. doi: [10.3354/esr01137](#)
- Read AJ, Barco S, Bell J, Borchers DL, Burt ML, Cummings EW, Dunn J, Fougères EM, Hazen L, Hodge LEW, Laura A-M, McAlarney RJ, Peter N, Pabst DA, Paxton CGM, Schneider SZ, Urian KW, Waples DM, McLellan WA (2014) [Occurrence, distribution and abundance of cetaceans in Onslow Bay, North Carolina, USA.](#) *Journal of Cetacean Research and Management* 14:23–35.

- Redfern JV, Kryc KA, Weiss L, Hodge BC, O'Brien O, Kraus SD, Quintana-Rizzo E, Auster PJ (2021) Opening a Marine Monument to Commercial Fishing Compromises Species Protections. *Front Mar Sci* 8:645314. doi: [10.3389/fmars.2021.645314](https://doi.org/10.3389/fmars.2021.645314)
- Roberts JJ, Best BD, Mannocci L, Fujioka E, Halpin PN, Palka DL, Garrison LP, Mullin KD, Cole TVN, Khan CB, McLellan WA, Pabst DA, Lockhart GG (2016) Habitat-based cetacean density models for the U.S. Atlantic and Gulf of Mexico. *Scientific Reports* 6:22615. doi: [10.1038/srep22615](https://doi.org/10.1038/srep22615)
- Roberts JJ, Yack TM, Halpin PN (2023) Marine mammal density models for the U.S. Navy Atlantic Fleet Training and Testing (AFTT) study area for the Phase IV Navy Marine Species Density Database (NMSDD), Document Version 1.3. Duke University Marine Geospatial Ecology Lab, Durham, NC
- Ryan C, Boisseau O, Cucknell A, Romagosa M, Moscrop A, McLanaghan R (2013) [Final report for trans-Atlantic research passages between the UK and USA via the Azores and Iceland, conducted from R/V Song of the Whale 26 March to 28 September 2012](#). Marine Conservation Research International, Essex, UK
- Schick R, Halpin P, Read A, Urban D, Best B, Good C, Roberts J, LaBrecque E, Dunn C, Garrison L, Hyrenbach K, McLellan W, Pabst D, Palka D, Stevick P (2011) Community structure in pelagic marine mammals at large spatial scales. *Marine Ecology Progress Series* 434:165–181. doi: [10.3354/meps09183](https://doi.org/10.3354/meps09183)
- Stone KM, Leiter SM, Kenney RD, Wikgren BC, Thompson JL, Taylor JKD, Kraus SD (2017) Distribution and abundance of cetaceans in a wind energy development area offshore of Massachusetts and Rhode Island. *J Coast Conserv* 21:527–543. doi: [10.1007/s11852-017-0526-4](https://doi.org/10.1007/s11852-017-0526-4)
- Whitt AD, Powell JA, Richardson AG, Bosyk JR (2015) [Abundance and distribution of marine mammals in nearshore waters off New Jersey, USA](#). *Journal of Cetacean Research and Management* 15:45–59.